

Near-extremal hydrodynamics and the holographic product formula

Edwan Préau^a

^b*Institute for Theoretical Physics and Center for Extreme Matter and Emergent Phenomena,
Utrecht University, 3584 CC Utrecht, The Netherlands*

E-mail: e.c.m.preau@uu.nl

ABSTRACT: The holographic product formula is used to determine the general form taken by holographic spectral functions in the near-extremal hydrodynamic regime, with energy ω , momentum k and temperature T much smaller than a hard scale μ . The resulting expressions simplify in the extremal limit $T \ll \omega, k \ll \mu$, for which the low-temperature gapless modes and the IR conformal behavior factorize. In some cases, this factorization extends to the general near-extremal regime $\omega, k, T \ll \mu$ at leading order in T/μ . Several examples are discussed with different types of gapless modes and IR CFTs, including new numerical results for low temperature quasi-normal modes. We end with a concrete application that shows how the inclusion of the IR conformal behavior improves the description of the spectral function at low energies.

Contents

1	Introduction and summary	2
2	The product formula	4
2.1	The formula	4
2.2	Application to near-extremal hydrodynamics	6
2.3	Special behavior of the soft poles	9
3	Examples of product formulae	10
3.1	Probe current correlators	10
3.1.1	(Near-)extremal hydrodynamic limit	12
3.2	Stress-tensor correlators in the sound channel	14
3.3	Magnetized branes	19
4	An application to holographic neutrino transport	22
5	Discussion	24
A	IR limit of near-extremal correlators	26
B	An example at next-to-leading order in the near-extremal hydrodynamic expansion	27
C	Correlators for different field variables in the probe longitudinal gauge sector	29
D	Poles of the probe current correlators	31
D.1	Transverse correlator	31
D.2	Longitudinal correlator	31
E	Coefficients of the helicity-0 fluctuation equations	32
F	Stress-tensor correlators for other numbers of dimensions	33
F.1	$n = 2$	33
F.2	$n \geq 4$	34
G	Poles of the stress-tensor correlators	35
G.1	Diffusive channel	35
G.2	Sound channel	35
H	Scalar poles of the magnetic black brane	36

1 Introduction and summary

Most finite temperature field theories are described by hydrodynamics over long times and distances. That is, for energies ω and momenta k much smaller than temperature T , the dynamics of most systems reduces to the conservation equations for their conserved currents. This includes in particular the majority of holographic theories, whose gravitational dual should therefore also admit a fluid description in the hydrodynamic regime. This result was established explicitly in [1], and has been called the *fluid/gravity correspondence*.

A more surprising result that has since been observed in holographic systems at finite density, is that hydrodynamics seemingly continues to hold in the low temperature limit $T \ll \mu$ (with μ the chemical potential), as long as energies and momenta remain much smaller than μ [2–8]. In particular, at leading order in the low ω, k expansion, holographic two-point functions were found to agree with the zero-temperature limit of hydrodynamic correlators [4, 5]. Not only do the hydrodynamic poles survive, but no sign was found at this order of the branch cut that is known to arise at $T = 0$ [9, 10], which is related to the lower-dimensional conformal field theory (CFT) emerging in the infra-red (IR) of these holographic systems.

The recent calculation of [11] at next-to-leading order made it clear that the branch cut puzzle only exists at leading order, since the next order already contains logarithmic signatures of the branch cut. However, the result of [11] still does not contain a clear imprint from the IR CFT.

In this work, we exploit the special analytic properties of holographic correlators to get more insight into their structure in the near-extremal hydrodynamic regime $\omega, k, T \ll \mu$. Specifically, we derive the consequences of the recently established holographic product formula [12], which makes it possible to express holographic spectral functions as a product over their poles. This formula therefore allows to write the general form of near-extremal holographic correlators based on their known pole structure, which features three types of poles (see figure 1): the hard poles with gaps of order $\mathcal{O}(\mu)$, the soft poles with gaps of order $\mathcal{O}(T)$ (related to the IR CFT), and the gapless poles, which behave like hydrodynamic modes at leading order in the near-extremal hydrodynamic limit. From this structure, we deduce the *near-extremal hydrodynamic product formula*

$$\rho(\omega, k) = \sinh\left(\frac{\omega}{2T}\right) \frac{\gamma(\omega, k) \mathcal{G}_s(\omega, k)}{\prod_{n \in \text{gapless}} (\omega^2 - \omega_n^2)(\omega^2 - (\omega_n^*)^2)},$$

with ρ the spectral function, \mathcal{G}_s the product over the soft poles and γ a generalized susceptibility, which is analytic in ω for $\omega \ll \mu$.

Due to the close relation between the soft poles and the poles of the IR CFT correlator, it is expected that \mathcal{G}_s should also somehow be related to the IR correlator \mathcal{G}_{IR} . However, it is not true that \mathcal{G}_s and \mathcal{G}_{IR} are equal in the general near-extremal hydrodynamic regime, which makes the above product formula of limited use in general. Instead, the product formula is most useful in the limit of vanishing temperature – i.e. for $T \ll \omega, k \ll \mu$ – where the soft poles merge into a branch cut, and the low ω behavior of ρ can be shown to be controlled by the IR CFT_q: $\rho \sim (\omega^2 - \vec{k}_{q-1}^2)^{\Delta(k)-q/2}$, with $\Delta(k)$ the momentum-dependent

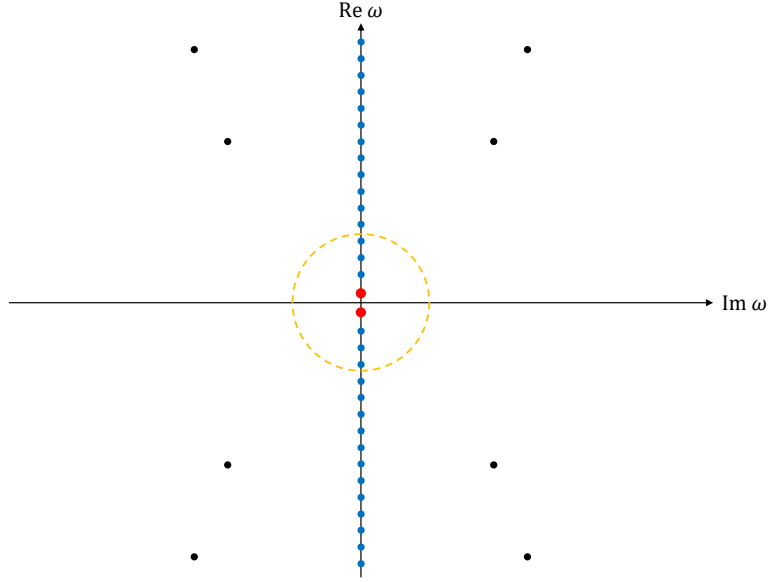


Figure 1: Schematic pole structure of holographic spectral functions in the near-extremal regime $T \ll \mu$. The black dots indicate hard poles of order $\mathcal{O}(\mu)$, the blue dots soft poles of order $\mathcal{O}(T)$ and the red dot is an example of gapless pole. The near-extremal hydrodynamic region (bounded by the yellow-dashed line) contains only soft and gapless poles. This picture is close to the actual pole structure of the correlators in section 3.2, but more general behaviors are possible. In particular the soft poles of section 3.3 have finite real parts.

IR conformal dimension and \vec{k}_{q-1} the spatial momentum along the IR CFT directions. From this, we infer the *extremal hydrodynamic product formula*

$$\rho = \frac{\gamma(\omega, k)(\omega^2 - \vec{k}_{q-1}^2)^{\Delta(k)-q/2}}{\prod_{n \in \text{gapless}} (\omega^2 - \omega_n^2)(\omega^2 - (\omega_n^*)^2)},$$

where γ is finite at $\omega = 0$, and is expected to follow a generalized (non-local) hydrodynamic expansion for $\omega, k \ll \mu$, including a mixture of polynomial and logarithmic terms.

In some cases, the soft poles can be shown (numerically) to precisely approach the IR poles in the near-extremal limit, up to corrections of order $\mathcal{O}(T/\mu)$ [2, 6]. In these cases, the near-extremal product formula simplifies at leading order in T/μ to

$$\rho = \sinh\left(\frac{\omega}{2T}\right) \frac{\tilde{\gamma}(\omega, k)\mathcal{G}_{\text{IR}}(\omega, k)}{\prod_{n \in \text{gapless}} (\omega^2 - \omega_n^2)(\omega^2 - (\omega_n^*)^2)} (1 + \mathcal{O}(T/\mu)),$$

with \mathcal{G}_{IR} the thermal correlator in the IR CFT, and $\tilde{\gamma}$ analytic in ω . This expression is valid in the general near-extremal hydrodynamic regime, including when ω is of the same order as the temperature.

The last two product formulae are the main results emphasized in this work. Whenever they apply, these formulae imply a simple factorized structure for holographic spectral functions in the (near-)extremal hydrodynamic limit, where both the low-temperature gapless modes and the IR conformal behavior appear explicitly.

The rest of this paper is organized as follows. Section 2 discusses in more details the developments summarized above, whereas section 3 presents several examples where the product formula can be used to determine the general structure of near-extremal spectral functions. This includes probe gauge field (section 3.1) and helicity-0¹ metric (section 3.2) perturbations on the AdS₅-Reissner-Nordström background – with a (0+1)-dimensional CFT in the IR – as well as scalar perturbations of magnetized black branes (section 3.3), whose IR description is in terms of a (1+1)-dimensional CFT [10, 14]. As intermediate results, we computed numerically the low-lying poles of the spectral functions in the near-extremal regime for all three cases. These numerical results are presented in appendices D, G and H.

Section 4 discusses a concrete application of the product formula to the problem analyzed in [7], related to neutrino transport in dense holographic matter. Improving the hydrodynamic approximation to the weak-current correlators with the IR scaling is shown to give a better description of the neutrino opacity near the Fermi surface (see figure 3).

Several additional details are provided in the appendices. In particular, in appendix B, we show how the next-to-leading order result of [11] is consistent with the product formula, which completes it at low energy ω by having the IR power-law appear explicitly.

2 The product formula

We present in this section the product formula for holographic two-point functions, as introduced in [12]. We first review the formula and its conditions of application, and then work out its consequences for the structure of holographic correlators in the near-extremal regime.

2.1 The formula

The product formula [12] is a statement about thermal two-point functions at equilibrium. For a given operator \mathcal{O} , it is best expressed in terms of the two-sided correlator G_{12} , defined in position space as

$$G_{12}(t, \vec{x}) \equiv \frac{1}{Z(\beta)} \text{Tr} \left[e^{-\beta H} \mathcal{O} \left(t - \frac{i\beta}{2}, \vec{x} \right) \mathcal{O}(0, 0) \right], \quad (2.1)$$

with $\beta \equiv 1/T$ the inverse temperature, H the Hamiltonian and $Z(\beta) \equiv \text{Tr}[e^{-\beta H}]$ the partition function. G_{12} corresponds to the Wightman function, but evaluated with an imaginary time shift $-i\beta/2$.

At equilibrium, the Wightman function is related to the retarded correlator

$$G_R(t, \vec{x}) \equiv i\theta(t) \frac{1}{Z(\beta)} \text{Tr} \left(e^{-\beta H} [\mathcal{O}(t, \vec{x}), \mathcal{O}(0, 0)] \right), \quad (2.2)$$

¹The helicity-1 shear-channel of metric perturbations has been analyzed in the recent work [13].

which may be written in Fourier space as

$$G_{12}(\omega, \vec{k}) = \frac{\text{Im}G_R(\omega, \vec{k})}{\sinh(\beta\omega/2)} \equiv \frac{G_R(\omega, \vec{k}) - G_R(-\omega, \vec{k})}{2i \sinh(\beta\omega/2)}, \quad (2.3)$$

with ω the energy and \vec{k} the spatial momentum².

Now the product formula expresses certain holographic two-sided thermal correlators in Fourier space as a product over their poles $\omega_n(\vec{k})$ ³

$$G_{12}(\omega, \vec{k}) = \frac{\gamma(\vec{k})}{\prod_{n=1}^{\infty} \left(1 - \frac{\omega^2}{\omega_n(\vec{k})^2}\right) \left(1 - \frac{\omega^2}{(\omega_n^*(\vec{k}))^2}\right)}, \quad (2.4)$$

with $\gamma(\vec{k})$ free of zeroes and poles. Note in particular that the residues do not appear explicitly in the formula, and their data is fully captured by the poles and the function $\gamma(\vec{k})$. Equation (2.4) is a consequence of Hadamard's factorization theorem, which applies as long as $G_{12}(\omega)$ is meromorphic (its only singularities are isolated poles), has no zeroes⁴, and behaves asymptotically as

$$\left|G_{12}(\omega, \vec{k})\right|_{|\omega| \rightarrow \infty} \sim e^{-\lambda(\theta)|\omega|}, \quad \lambda(\theta) \geq 0, \quad \omega \equiv |\omega|e^{i\theta}, \quad (2.5)$$

implying that $1/G_{12}(\omega)$ is an entire function of order 1 [12].

Meromorphicity and the asymptotic behavior (2.5) are generic properties of holographic correlators [15–17]. The property that is not generically obeyed is for the correlator to be free of zeroes. It can be shown to be the case upon two conditions [12]:

- It should be possible to write the dual fluctuation equations as decoupled and in the Schrödinger form

$$\psi''(z) + (\omega^2 - V(z))\psi(z) = 0, \quad (2.6)$$

with z the tortoise coordinate, for which the background AdS black-hole metric takes the form

$$ds^2 = e^{2A(z)}(-f(z)dt^2 + dz^2 + ds_{d-1}^2), \quad (2.7)$$

with $A(z)$ the scale factor, $f(z)$ the blackening function and ds_{d-1}^2 the metric along the spatial directions of the d -dimensional boundary.

A given set of decoupled fluctuation equations can always be written in the Schrödinger form (2.6) upon appropriate field redefinitions (see e.g. appendix B of [18]). However, finding variables that obey decoupled equations is more difficult in general, and not

²This relation holds when there is no chemical potential for the charges of the operator \mathcal{O} . Otherwise ω should be shifted by the appropriate chemical potentials μ in the argument of the sinh (rescaling also G_{12} by a factor $e^{-\beta\mu/2}$).

³In the special case of purely imaginary poles, there is a single factor $(1 - (\omega/\omega_n)^2)$.

⁴The extension of the product formula to the case where the two-sided correlator would admit a discrete set of zeroes (as a function of ω) is obtained by a straightforward multiplication by the appropriate factors in the numerator $\prod_{m \in \text{zeroes}} (1 - \omega/\omega_m)$.

always possible⁵. A non-trivial example of such variables is given by the “master fields” for the metric and gauge fields fluctuations of the RN background [2, 3, 19];

- The potential $V(z)$ should be regular for all $z > 0$, with boundary ($z \rightarrow 0$) and horizon ($z \rightarrow \infty$) asymptotics obeying

$$V(z) \underset{z \rightarrow 0}{\sim} \frac{\nu^2 - \frac{1}{4}}{z^2} \quad , \quad z^2 V(z) \underset{z \rightarrow \infty}{\rightarrow} 0, \quad (2.8)$$

with $\nu^2 \geq 0$. In practice, all regular holographic solutions obey the IR condition at finite temperature, with $V(z) \sim e^{-4\pi z/\beta}$ for $z \rightarrow \infty$ [12]. The UV z^{-2} behavior of the potential is also generic, although in some cases the parameter ν^2 may become negative. So the effective condition on the potential is the absence of singularities in the bulk – i.e. for all $z \in (0, \infty)$ – together with $\nu^2 \geq 0$.

Note that, even though it will be important for the developments of this work that the fluctuation equations decouple, it is most of the time not crucial that G_{12} is actually free of zeroes. In other words, most of our results still apply for a Schrödinger potential that admits singularities. In this case the generalized susceptibilities introduced below may admit zeroes. There is one exception in subsection 2.3 where we mention explicitly that the no-zeroes conditions should hold.

2.2 Application to near-extremal hydrodynamics

We now consider a thermal state with a dimensionful source parameter μ , in the near-extremal limit $T \ll \mu$, such that the bulk dual corresponds to a near-extremal black brane with AdS_p -Schwarzschild near-horizon geometry. The low energy excitations of such states are described by a CFT_{p-1} at each point in the transverse space of dimension $d - p + 1$ [9, 14]. In momentum space, this translates into a family of $(p - 1)$ -dimensional CFT’s labeled by the transverse momentum \vec{k}_{d-p+1} . Examples with $p = 2$ include the charged AdS Reissner-Nordström (RN) black brane, with μ the chemical potential, and the neutral solution of [20, 21], with μ the source for the translation-symmetry breaking axions. The magnetized CFT₂ of [14] is an example with $p = 3$, where μ is related to the magnetic field via $\mu = \sqrt{B}$.

The black brane metrics may be written in conformal coordinates as

$$ds^2 = e^{2A(r)} \left(-f(r)dt^2 + f(r)^{-1}dr^2 + ds_{d-1}^2 \right), \quad (2.9)$$

with $A(r)$ the scale factor and $f(r)$ the blackening function. $f(r)$ vanishes at the horizon radius r_H , which is a function of T and μ . In the near-extremal limit, r_H approaches its extremal value

$$r_H(T, \mu) = r_e(\mu) \left(1 + \mathcal{O}\left(\frac{T}{\mu}\right) \right), \quad (2.10)$$

⁵Another possible issue may be that, even though the product formula applies to the correlators dual to the decoupled variables, it does not carry over to the original correlators of interest. This typically arises when the relation between the two types of correlators is non-linear, as in the example presented in appendix F.

where the extremal radius r_e is proportional to μ^{-1} .

We now consider two-sided correlators on these black brane geometries, in a specific low energy regime

$$|\omega|, |\vec{k}|, T \ll r_e^{-1}, \quad (2.11)$$

that we call *near-extremal hydrodynamics*. In this regime, the poles of the correlators may be divided into three categories (see figure 1 for an illustration):

- Hard poles $\Omega_n(\vec{k}) = \mathcal{O}(r_e^{-1})$;
- Soft poles $\omega_n^s(\vec{k}) = \mathcal{O}(T)$;
- Gapless poles $\omega_n^g(\vec{k})$, which go to zero at zero momentum. Such poles were exhibited in [2–5]. They do not go to zero in the limit of vanishing temperature⁶, where they instead follow a dispersion relation which at leading order in momentum is similar to hydrodynamic modes⁷ (e.g. a sound mode $\omega^g(\vec{k}) \sim c_s |\vec{k}| - i\Gamma \vec{k}^2 + \mathcal{O}(r_e^3 \vec{k}^4)$ [3, 4] or diffusive mode $\omega^g(\vec{k}) \sim -iD \vec{k}^2 + \mathcal{O}(r_e^3 \vec{k}^4)$ [2, 4, 5]).

Now, if we were in the standard hydrodynamic regime

$$|\omega|, |\vec{k}| \ll T \ll r_e^{-1}, \quad (2.12)$$

the correlators would be dominated by the gapless (hydrodynamic) poles, whereas the product over the hard and soft poles in (2.4) would be effectively analytic, and resum into the residues of the hydrodynamic poles

$$\begin{aligned} G_{12}(\omega, \vec{k}) &= \frac{\gamma(\vec{k})}{\prod_{n \in \text{gapless}} \left(1 - \frac{\omega^2}{\omega_n^g(\vec{k})^2}\right) \left(1 - \frac{\omega^2}{(\omega_n^{g*}(\vec{k}))^2}\right)} \times \\ &\quad \times \frac{1}{\prod_{n=1}^{\infty} \left(1 - \frac{\omega^2}{\omega_n^s(\vec{k})^2}\right) \left(1 - \frac{\omega^2}{(\omega_n^{g*}(\vec{k}))^2}\right) \prod_{n=1}^{\infty} \left(1 - \frac{\omega^2}{\Omega_n(\vec{k})^2}\right) \left(1 - \frac{\omega^2}{(\Omega_n^*(\vec{k}))^2}\right)} \\ &= \frac{\tilde{\gamma}(\omega, \vec{k})}{\prod_{n \in \text{gapless}} \left(\omega^2 - \omega_n^g(\vec{k})^2\right) \left(\omega^2 - (\omega_n^{g*}(\vec{k}))^2\right)}, \end{aligned} \quad (2.13)$$

with $\tilde{\gamma}$ analytic for $|\omega|, |\vec{k}| \ll T$.

By contrast, in the general near-extremal limit (2.11), both gapless and soft poles contribute to the effective correlator

$$G_{12}(\omega, \vec{k}) = \frac{\tilde{\gamma}_e(\omega, \vec{k}) \mathcal{G}_{12}^s(\omega, \vec{k})}{\prod_{n \in \text{gapless}} \left(\omega^2 - \omega_n^g(\vec{k})^2\right) \left(\omega^2 - (\omega_n^{g*}(\vec{k}))^2\right)}, \quad (2.14)$$

⁶With this definition, the results of [6] indicate that the gapless poles (and the soft poles) are generically discontinuous as a function of momentum near a collision with a soft pole. The discontinuities are small, of order $\mathcal{O}(r_e T)$.

⁷Because of this similarity, and following the terminology of [22], a possible name for these modes would be “quantum hydrodynamic modes”. They clearly differ from standard hydrodynamic modes since they contain non-analytic logarithmic terms at higher order in $r_e |\vec{k}|$ [11].

where $\tilde{\gamma}_e$ is analytic in ω for $|\omega|, |\vec{k}| \ll r_e^{-1}$, and we defined the soft factor as

$$\mathcal{G}_{12}^s(\omega, \vec{k}) \equiv \frac{1}{\prod_{n=1}^{\infty} \left(1 - \frac{\omega^2}{\omega_n^s(\vec{k})^2}\right) \left(1 - \frac{\omega^2}{(\omega_n^{s*}(\vec{k}))^2}\right)}. \quad (2.15)$$

At this point it is interesting to consider the limit $T \rightarrow 0$, for which the structure of the soft sector (2.15) is expected to simplify. For $|\omega|, |\vec{k}| \ll r_e^{-1}$ and away from gapless poles, holographic near-extremal correlators computed from (2.6) can indeed be shown to be proportional to the corresponding IR correlators [9, 10]⁸

$$G_{12}(\omega, \vec{k}) = a(\vec{k}) \mathcal{G}_{12}(\omega, \vec{k}) \left(1 + \mathcal{O}(r_e \omega, r_e^2 \vec{k}^2) + \text{gapless poles corrections}\right), \quad (2.16)$$

with \mathcal{G}_{12} the two-sided correlator in the IR CFT_{p-1}, and $a(\vec{k})$ some function of the momentum. At zero temperature, the IR correlator is constrained by conformal symmetry to take the form

$$\mathcal{G}_{12}(\omega, \vec{k}) = \frac{\mathcal{C}(\vec{k}_{d-p+1})}{\sinh(\beta \omega/2)} (r_e^2(\omega^2 - \vec{k}_{p-2}^2))^{\Delta(\vec{k}_{d-p+1}) - (p-1)/2}, \quad (2.17)$$

where the sinh comes from (2.3), and we split the spatial momentum into the part that is along the CFT direction \vec{k}_{p-2} and the transverse part \vec{k}_{d-p+1} . $\Delta(\vec{k}_{d-p+1})$ is the IR conformal dimension associated to G_{12} . For generic values of the momentum, Δ is not an integer, which implies that the correlator G_{12} has branch points at $\omega = \pm|\vec{k}_{p-2}|$ (there is a single branch point at $\omega = 0$ for $p = 2$). This means that the soft poles merge into branch cuts in the zero-temperature limit [9].

From the above observations, we deduce that for $T \rightarrow 0$, the soft factor (2.15) should become free of poles, with branch points instead at $\omega = \pm|\vec{k}_{p-2}|$, near which the numerator of (2.14) behaves as

$$\tilde{\gamma}_e(\omega, \vec{k}) \mathcal{G}_{12}^s(\omega, \vec{k}) = \frac{\tilde{a}(\vec{k})}{\sinh(\beta \omega/2)} (r_e^2(\omega^2 - \vec{k}_{p-2}^2))^{\Delta(\vec{k}_{d-p+1}) - (p-1)/2} \left(1 + \mathcal{O}(r_e \omega, r_e^2 \vec{k}^2)\right). \quad (2.18)$$

Note that, unlike (2.16), the series in (2.18) is expected to remain well defined for any (ω, \vec{k}) such that $r_e|\omega|, r_e|\vec{k}| \ll 1$. In particular, the expansion does not break down when ω approaches gapless poles, since the latter have been factored out in (2.14). However, due to the presence of the branch points, typical terms in the series will contain logarithms, where both $\log(r_e^2(\omega^2 - \vec{k}_{p-2}^2))$ and $\log(r_e^2 \vec{k}_{d-p+1}^2)$ may in principle appear (appendix B gives an example with $p = 2$). Finally, rewriting (2.18) in terms of a generalized susceptibility $\gamma_e(\omega, \vec{k})$, and using (2.3), for $|\omega|, |\vec{k}| \gg T$ the product formula (2.14) may be written as

$$\text{Im}G_R(\omega, \vec{k}) = \frac{\gamma_e(\omega, \vec{k}) (r_e^2(\omega^2 - \vec{k}_{p-2}^2))^{\Delta(\vec{k}_{d-p+1}) - (p-1)/2}}{\prod_{n \in \text{hydro}} \left(\omega^2 - \omega_n^h(\vec{k})^2\right) \left(\omega^2 - (\omega_n^{h*}(\vec{k}))^2\right)}. \quad (2.19)$$

⁸We generalize the results of [9, 10] to general near-extremal black holes in appendix A. Here we are considering the regime where not only $r_e|\omega|$ but also $r_e|\vec{k}|$ is small.

In the following, we refer to (2.19) as the *extremal hydrodynamic product formula*.

The product formula (2.19) thus exhibits an interesting structure for the two-sided correlator, where both the gapless poles and the non-analytic IR behavior appear explicitly, moreover in a simple, factorized form. The gapless poles and the generalized susceptibility γ_e are expected to admit expansions as generalized hydrodynamic series, including both integer powers and logarithms of energy and momentum.

In particular, it is an important aspect of (2.19) that it allows to extend the near-extremal hydrodynamic expansion to the region near the branch points. In a standard expansion, the power-law (2.18) would indeed be expanded at low momentum, generating terms of the form⁹ $\vec{k}_{d-p+1}^{2m} \log(\omega^2 - \vec{k}_{p-2}^2)$, which imply a breakdown of the expansion at the branch points. The leading behavior of the numerator (2.18) resums all such terms, which allows to include the branch points in the near-extremal hydrodynamic regime. Section 4 gives a concrete example of this IR improvement in the case of $p = 2$.

Another comment is related to the number of gapless poles that appear in the denominator of (2.14), which may actually depend on the order of the hydrodynamic expansion. Appendix B gives an example of this, where the single leading order diffusive mode $\omega_D(\vec{k}) = -iD\vec{k}^2$, splits into two poles with finite real parts at next-to-leading order [11]. In this case $\gamma_e(\omega, \vec{k})$ should have zeroes at the appropriate order to account for the pole merging.

2.3 Special behavior of the soft poles

In some cases, numerical results show that the soft poles approach precisely the IR poles in the extremal limit $r_e T \rightarrow 0$

$$\omega_n^s(\vec{k}) = \omega_n^{\text{IR}}(\vec{k}) (1 + \mathcal{O}(r_e T)) , \quad (2.20)$$

where ω_n^{IR} are the poles of the IR CFT_{p-1} correlator \mathcal{G}_{12} . Examples of this behavior for $p = 2$ are given in [2, 6, 8, 23, 24] (with [11] being a counter-example), whereas section 3.3 describes an example with $p = 3$. Based on known examples, it looks like (2.20) typically holds either for correlators that do not have gapless poles (e.g. the transverse current in section 3.1 or the scalar in section 3.3), or that couple to energy and momentum (e.g. the correlators of section 3.2).

When (2.20) holds, for all ω far enough from the IR poles, the soft factor (2.15) can be directly expressed in terms of \mathcal{G}_{12} . This can be seen from the fact that \mathcal{G}_{12} itself is a holographic thermal correlator for which a product formula (2.4) may be written

$$\mathcal{G}_{12}(\omega, \vec{k}) = \frac{\mathcal{K}(\vec{k})}{\prod_{n=1}^{\infty} \left(1 - \frac{\omega^2}{\omega_n^{\text{IR}}(\vec{k})^2}\right) \left(1 - \frac{\omega^2}{(\omega_n^{\text{IR}*}(\vec{k}))^2}\right)} , \quad (2.21)$$

with $\mathcal{K}(\vec{k})$ non-zero. Note that here it is important that the IR correlator is actually free of zeroes¹⁰. Then, if ω is such that for all IR modes $|\omega - \omega_n^{\text{IR}}|/T \gg r_e T$ (including in particular

⁹An example is given by the result of [11] discussed in appendix B, which contains the first term in this expansion.

¹⁰Since the IR correlator can be computed from the $z \rightarrow \infty$ limit of the fluctuation equation (2.6) (see appendix A), it is clear that if \mathcal{G}_{12} obeys the no-zeroes conditions, then so does \mathcal{G}_{12} .

physical energies $\omega \in \mathbb{R}$), then the product over the soft poles can be approximated in the near-extremal limit by

$$\frac{1}{\prod_{n=1}^{\infty} \left(1 - \frac{\omega^2}{\omega_n^s(\vec{k})^2}\right) \left(1 - \frac{\omega^2}{(\omega_n^{s*}(\vec{k}))^2}\right)} = \mathcal{K}(\vec{k})^{-1} \mathcal{G}_{12}(\omega, \vec{k}) (1 + \mathcal{O}(r_e T)). \quad (2.22)$$

Substituting into (2.14), and defining $\tilde{\gamma}_e(\omega, \vec{k}) \equiv \gamma_e(\omega, \vec{k})/\mathcal{K}(\vec{k})$, makes the low-energy correlator directly appear in the expression of G_{12}

$$G_{12}(\omega, \vec{k}) = \frac{\tilde{\gamma}_e(\omega, \vec{k})}{\prod_{n \in \text{gapless}} \left(\omega^2 - \omega_n^g(\vec{k})^2\right) \left(\omega^2 - (\omega_n^{g*}(\vec{k}))^2\right)} \mathcal{G}_{12}(\omega, \vec{k}) (1 + \mathcal{O}(r_e T)), \quad (2.23)$$

which is valid for all ω outside small disks of radius of order $\mathcal{O}(r_e T)$ around the IR poles. The generalized susceptibility $\tilde{\gamma}_e(\omega, \vec{k})$ is analytic in ω in the near-extremal hydrodynamic regime (2.11).

In the general near-extremal regime (2.11), $\mathcal{G}_{12}(\omega, \vec{k})$ is the two sided correlator in the IR CFT_{p-1} at finite temperature. This makes equation (2.23) particularly useful in the case of $p = 2$ and 3 , since the general expression of thermal two-point functions is known for one-dimensional and two-dimensional CFT's (see e.g. [9] and [12, 25]). In these cases, the soft factor (2.22) can therefore be expressed at leading order in $r_e T$ in an exact analytic form (up to a \vec{k} -dependent factor), including for energies $|\omega| \lesssim T$.

This concludes the general presentation of the near-extremal hydrodynamic product formula. The next section discusses some concrete examples.

3 Examples of product formulae

We present in this section several examples where the product formula applies and provides useful expressions for different types of holographic correlators. This includes cases with different gapless modes – both diffusive (section 3.1) and sound modes (section 3.2) – and for different values of p : $p = 2$ (sections 3.1 and 3.2) and $p = 3$ (section 3.3).

3.1 Probe current correlators

We consider here a first example, corresponding to gauge field fluctuations A_μ , which obey the Maxwell equations

$$\partial_M (\sqrt{-g} F^{MN}) = 0, \quad F_{MN} \equiv \partial_M A_N - \partial_N A_M, \quad (3.1)$$

on top of the Reissner-Nordström background¹¹ with metric

$$ds^2 = \frac{\ell^2}{r^2} \left(-f(r) dt^2 + f(r)^{-1} dr^2 + d\vec{x}^2 \right), \quad (3.2)$$

where the blackening function $f(r)$ vanishes at the horizon radius r_H .

¹¹All results in this section are actually independent of the blackening function $f(r)$, as long as it admits an AdS₂ IR geometry in the near-extremal limit.

The operator dual to A_μ is a conserved current J^μ , with vanishing background density $\langle J^0 \rangle = 0$, and not charged under any other background density. This corresponds to the correlators studied in [7], that are related to neutrino transport.

At finite momentum \vec{k} , the perturbations split into transverse and longitudinal modes, such that the Fourier space current-current correlator may be written as

$$\langle J_\mu J_\nu \rangle (\omega, \vec{k}) = P_{\mu\nu}^\perp(\omega, \vec{k}) i\Pi^\perp(\omega, \vec{k}) + P_{\mu\nu}^\parallel(\omega, \vec{k}) i\Pi^\parallel(\omega, \vec{k}), \quad (3.3)$$

with the non-zero components of the transverse and longitudinal projectors respectively given by

$$P_{ij}^\perp(\omega, \vec{k}) = \delta_{ij} - \frac{k_i k_j}{\vec{k}^2}. \quad (3.4)$$

$$P_{tt}^\parallel(\omega, \vec{k}) = \frac{\vec{k}^2}{\omega^2 - \vec{k}^2}, \quad P_{ti}^\parallel(\omega, \vec{k}) = -\frac{\omega k^i}{\omega^2 - \vec{k}^2}, \quad P_{ij}^\parallel(\omega, \vec{k}) = \frac{\omega^2}{\omega^2 - \vec{k}^2} \frac{k_i k_j}{\vec{k}^2}. \quad (3.5)$$

The polarization functions Π^\perp and Π^\parallel may be computed by solving the decoupled Maxwell equations for the two types of modes

$$\partial_r \left(\frac{f(r)}{r^{d-3}} \partial_r A_i^\perp \right) + \frac{1}{r^{d-3} f(r)} \left(\omega^2 - f(r) \vec{k}^2 \right) A_i^\perp = 0, \quad (3.6)$$

$$\partial_r \left(\frac{f(r)}{r^{d-3} (\omega^2 - f(r) \vec{k}^2)} \partial_r E^\parallel \right) + \frac{1}{r^{d-3} f(r)} E^\parallel = 0, \quad (3.7)$$

where $d \geq 3$ is the boundary dimension¹² and the transverse gauge field and longitudinal electric field are defined as

$$A_i^\perp \equiv A_i - \hat{k}_i \hat{k}^j A_j, \quad E^\parallel \equiv |\vec{k}| A_t + \omega \hat{k}^j A_j, \quad \hat{k}^i = \frac{k^i}{|\vec{k}|}. \quad (3.8)$$

Equations (3.6) and (3.7) are not in the Schrödinger form (2.6). (3.6) can be put in the appropriate form by going to tortoise coordinates and with a simple field redefinition

$$A_i^\perp(r) \rightarrow r(z)^{(d-3)/2} \psi^\perp(z), \quad \frac{dz}{dr} = \frac{1}{f(r)}, \quad (3.9)$$

which gives

$$\partial_z^2 \psi^\perp + (\omega^2 - V^\perp(z)) \psi^\perp(z) = 0, \quad (3.10)$$

$$V^\perp(z) = f(z) \vec{k}^2 + \frac{(d-3)(d-1)f(z)^2}{4r(z)^2} - \frac{(d-3)f'(z)}{2r(z)}. \quad (3.11)$$

The potential (3.11) is regular for $z \in (0, \infty)$, and its UV behavior is as in (2.8) with $\nu^2 = (d-2)^2/4 \geq 0$. The transverse two-sided polarization function is therefore free of zeroes.

¹²We focus on theories that feature diffusion, which excludes in particular (1+1)-dimensional CFT's [26, 27].

The longitudinal equation (3.7) can be put into the Schrödinger form with a different field redefinition

$$E^{\parallel}(r) \rightarrow \left(r(z)^{d-3} (\omega^2 - f(z) \vec{k}^2) \right)^{1/2} \psi^{\parallel}(z), \quad (3.12)$$

with the corresponding potential given by

$$\begin{aligned} V^{\parallel}(z) = & f(z) \vec{k}^2 + \frac{(d-3)(d-1)f(z)^2}{4r(z)^2} - \frac{(d-3)f'(z)}{2r(z)} - \frac{(d-3)\vec{k}^2 f(z) f'(z)}{2r(z) (\omega^2 - f(z) \vec{k}^2)} + \\ & + \frac{3\vec{k}^4 f'(z)^2}{4(\omega^2 - f(z) \vec{k}^2)^2} + \frac{\vec{k}^2 f''(z)}{2(\omega^2 - f(z) \vec{k}^2)}. \end{aligned} \quad (3.13)$$

This potential has a pole when $f(z) \vec{k}^2 = \omega^2$, which can be reached at finite z for $\omega^2/\vec{k}^2 < 1$. Also its UV asymptotics are such that $\nu^2 = (d-2)^2/4$, except when $\omega^2 = \vec{k}^2$, for which $\nu^2 = -3$. As a consequence, we expect the corresponding two-sided correlator to feature some zeroes for $\omega^2/\vec{k}^2 \leq 1$. It can be checked (see e.g. [7]) that the correlator associated with E^{\parallel} is the polarization function Π^{\parallel} in (3.3). In this case, it is therefore simple to understand why there is a zero: since the full correlator should not have a pole at $\omega^2 = \vec{k}^2$, and because Π^{\parallel} is multiplied by the longitudinal projector (3.4), it results that Π^{\parallel} should vanish when $\omega^2 = \vec{k}^2$.

We will now check that there is no other zero than $\omega^2 = \vec{k}^2$, which can be done by considering the field

$$\Psi(z) \equiv \frac{\partial_z E^{\parallel}}{r(z)^{(d-3)/2} (\omega^2 - f(z) \vec{k}^2)}. \quad (3.14)$$

The latter obeys

$$\Psi''(z) + (\omega^2 - V_{\Psi}(z)) \Psi(z) = 0, \quad (3.15)$$

$$V_{\Psi}(z) = f(z) \vec{k}^2 + \frac{(d-3)(d-5)f(z)^2}{4r(z)^2} + \frac{(d-3)f'(z)}{2r(z)}, \quad (3.16)$$

so the corresponding two-sided correlator G_{Ψ} is free of zeroes. Since G_{Ψ} is related to the two-sided polarization function as¹³

$$\Pi_{12}^{\parallel}(\omega, \vec{k}) = c_0(\omega^2 - \vec{k}^2) G_{\Psi}(\omega, \vec{k}), \quad (3.17)$$

with c_0 a constant, we find that the only zero of the polarization function is indeed at $\omega^2 = \vec{k}^2$.

3.1.1 (Near-)extremal hydrodynamic limit

In the limit $T \ll |\omega|, |\vec{k}| \ll r_e^{-1}$ (with r_e the extremal horizon radius), the extremal hydrodynamic product formula (2.19) applies to G_{Ψ} , with $p = 2$ and the IR scaling dimension given by

$$\Delta(\vec{k}) \equiv \frac{1}{2} + \frac{1}{2} \sqrt{1 + \frac{8\vec{k}^2}{\partial_r^2 f(r_H)}}. \quad (3.18)$$

¹³See appendix C for details.

At leading order in the near-extremal hydrodynamic expansion, there is a single gapless pole $\omega_D(\vec{k}) = -iD\vec{k}^2$, with $D = r_H/(d-2)$ the diffusion constant [5]. In this regime, the longitudinal spectral function may thus be written as

$$\text{Im}\Pi_R^{\parallel}(\omega, \vec{k}) = -(\omega^2 - \vec{k}^2) \frac{\sigma \omega^{2\Delta(\vec{k})-1}}{\omega^2 + D^2 \vec{k}^4}, \quad (3.19)$$

with σ the conductivity. The expression (3.19) corresponds to the standard hydrodynamic expression for a diffusive mode [7], improved with the appropriate IR power-law.

At next-to-leading order, the numerical analysis presented in appendix D indicates that ω_D splits into two hydrodynamic poles, much like in [11] (see (B.8)). At this order and higher, we therefore expect the polarization function to be described by an expression of the form (B.9) in the extremal hydrodynamic regime.

We now come back to the transverse correlator, which does not admit any zeroes nor gapless poles. In this case, the near-extremal product formula (2.14) therefore predicts that Π^{\perp} should factorize as

$$\Pi_{12}^{\perp}(\omega, \vec{k}) = \gamma(\omega, \vec{k}) \mathcal{G}_{12}^s(\omega, \vec{k}), \quad (3.20)$$

with γ analytic and free of zeroes, and \mathcal{G}_{12}^s the soft factor (2.15). A numerical analysis of the transverse fluctuation equation (3.10) further indicates that the scenario discussed in section 2.3 applies in this sector, with the soft poles approaching the IR poles in the limit $r_e T \rightarrow 0$ (see appendix D). The near-extremal transverse polarization function may thus be written in the form (2.23), i.e. an analytic factor times the IR AdS₂ correlator [9]

$$\mathcal{G}_{12}(\omega, \vec{k}) = (\pi T)^{2\Delta-1} \frac{\cos(\pi(\Delta-1))}{\pi} \frac{\Gamma(\frac{3}{2} - \Delta)}{\Gamma(\frac{1}{2} + \Delta)} \left| \Gamma\left(\Delta - \frac{i\omega}{2\pi T}\right) \right|^2. \quad (3.21)$$

Absorbing for convenience some of the \vec{k} -dependent terms in (3.21) into the analytic factor, we get

$$\Pi_{12}^{\perp}(\omega, \vec{k}) = -\sigma^{\perp}(\omega, \vec{k}) \frac{(2\pi T)^{2\Delta-1}}{2\pi} \left| \Gamma\left(\Delta - \frac{i\omega}{2\pi T}\right) \right|^2 (1 + \mathcal{O}(r_e T)), \quad (3.22)$$

with σ^{\perp} analytic in the near-extremal hydrodynamic regime.

In the extremal limit $|\omega| \gg T$, we recover the extremal hydrodynamic product formula

$$\text{Im}\Pi_R^{\perp}(\omega, \vec{k}) = -\sigma^{\perp}(\omega, \vec{k}) \omega^{2\Delta(\vec{k})-1}. \quad (3.23)$$

In particular, at leading order in the hydrodynamic expansion we get

$$\text{Im}\Pi_R^{\perp}(\omega, \vec{k}) = -\sigma \omega^{2\Delta(\vec{k})-1} (1 + \mathcal{O}(r_e \omega, r_e \vec{k}^2)), \quad (3.24)$$

where we used that the two polarization functions should be equal for $\vec{k} = 0$ to get $\sigma^{\perp}(0) = \sigma$, with σ the same conductivity that appears in the expression of the longitudinal correlator (3.19).

The leading order extremal hydrodynamic expressions (3.19) and (3.24) will be compared with the numerically computed exact correlators in section 4. Before that, the following subsections discuss other settings where the product formula gives interesting information about the structure of the correlator in the near-extremal hydrodynamic regime.

3.2 Stress-tensor correlators in the sound channel

We now consider the case of helicity-0 stress-tensor correlators on the Reissner-Nordström (RN) background, whose gapless sector is qualitatively different from the previous example, since it features two types of gapless modes: a diffusive-like mode $\omega_D(\vec{k}) = -iD\vec{k}^2 + \mathcal{O}(\vec{k}^4)$, and a sound-like mode $\omega_s(\vec{k}) = c_s|\vec{k}| - i\Gamma\vec{k}^2 + \mathcal{O}(\vec{k}^4)$ [3, 4, 28].

The background metric is given by

$$ds^2 = \frac{\ell^2}{r^2} (-f(r)dt^2 + f(r)^{-1}dr^2 + d\vec{x}^2), \quad (3.25)$$

$$f(r) = 1 - 2Mr^{n+1} + Q^2r^{2n}, \quad (3.26)$$

where $n \equiv d - 1 \geq 2$ is the number of spatial dimensions at the boundary, that are denoted $x^i = (x, y_1, \dots, y_{n-1})$. The RN solution also contains a background gauge field

$$A = \frac{q}{n-1} (r_H^{n-1} - r^{n-1}) dt, \quad (3.27)$$

with q proportional to the density for the current dual to A , and r_H the horizon radius.

The stress-tensor correlators are computed from the fluctuation equations for the appropriate modes of the metric g_{MN} , which couple to the fluctuations of the gauge field (3.27). These equations can be written in terms of two gauge-invariants [3, 19]

$$\mathcal{A}(r) \equiv r^{2-n}\partial_r\delta A_t + \frac{q}{2} \left(\delta g_t^t - \frac{n}{n-1}(\delta g_i^i - \delta g_x^x) \right), \quad (3.28)$$

$$\Phi(r) \equiv r^{-n/2} \left[\delta g_i^i - \delta g_x^x + \frac{(n-1)f(r)}{H(r)} r \partial_r \delta g_i^i \right], \quad (3.29)$$

where $\delta\varphi$ refers to a small fluctuation of the field φ , and we took the 3-momentum \vec{k} to lie in the x direction (without loss of generality); we also defined

$$H(r) \equiv r^2\vec{k}^2 - \frac{n}{2}rf'(r). \quad (3.30)$$

The fields \mathcal{A} and Φ obey [3, 19]

$$\begin{aligned} f(r)r^{2-n}\partial_r \left(\frac{f(r)}{r^{2-n}}\partial_r \mathcal{A} \right) + \left(\omega^2 - f(r)\vec{k}^2 - \frac{2n^2(n-1)\zeta(r)f(r)^2}{r^2H(r)} \right) \mathcal{A} \\ = n(n-1)f(r)r^{n/2-2}q \left(\frac{4H(r)^2 - nP_Z(r)}{4nH(r)} \Phi - f(r)r\partial_r \Phi \right), \end{aligned} \quad (3.31)$$

$$f(r)\partial_r(f(r)\partial_r\Phi) + (\omega^2 - V_S(r))\Phi = (n-1)\frac{Q^2}{q} \frac{f(r)P_S(r)}{H(r)^2} r^{3n/2-2} \mathcal{A}, \quad (3.32)$$

where the expressions for the coefficients $\zeta(r)$, $P_Z(r)$, $P_S(r)$ and $V_S(r)$ are listed in appendix E.

It is possible to further simplify the problem by introducing the following ‘‘master’’ variables¹⁴

$$\Phi_{\pm} \equiv \alpha_{\pm}(r)\Phi - \frac{Q}{q}r^{n/2-1}\mathcal{A}, \quad (3.33)$$

¹⁴Note the relations between our variables and those of Kodama-Ishibashi (KI) [19]

$$\mathcal{A} = \vec{k}^2\mathcal{A}_{\text{KI}} \quad , \quad \Phi = \frac{1}{n}\vec{k}^2\Phi_{\text{KI}},$$

where

$$\alpha_{\pm}(r) \equiv (n+1) \frac{M \pm \rho(\vec{k})}{4Q} - \frac{n}{2} Q r^{n-1} \quad , \quad \rho(\vec{k}) \equiv \sqrt{M^2 + \frac{4\vec{k}^2 Q^2}{(n+1)^2}}. \quad (3.34)$$

These variables obey decoupled equations

$$f(r) \partial_r (f(r) \partial_r \Phi_{\pm}) + (\omega^2 - V_{\pm}(r)) \Phi_{\pm} = 0, \quad (3.35)$$

where the potential V_{\pm} can be expressed as

$$\begin{aligned} V_{\pm}(r) = & \pm \frac{2Q}{(n+1)\rho(\vec{k})} \left\{ \alpha_{\pm}(r) V_S(r) + \right. \\ & + \frac{f(r)}{4nr^3 H(r)} \left[2n(n-1)Qr^n \left(n^2 r f'(r) \left(r f'(r) - 2(2n+1)f(r) \right) - \right. \right. \\ & - 4n(n-2)f(r)\vec{k}^2 r^2 + 4n^3(n+1)f(r)(f(r)-1) - 4\vec{k}^4 r^4 \left. \right) + \\ & + \frac{n}{2} r \alpha_{\mp}(r) \left(r f'(r) \left(n(5n(2-3n)+8)f(r) + 8\vec{k}^2 r^2 + 2n(n-2)r f'(r) \right) - \right. \\ & \left. \left. - 2f(r) \left((n-4)(n-2)\vec{k}^2 r^2 - 8n^2(n^2-1)(f(r)-1) \right) - 8\vec{k}^4 r^4 \right) \right\]. \end{aligned} \quad (3.36)$$

Equation (3.35) finally takes the Schrödinger form (2.6) if we use the tortoise coordinates z

$$\partial_z^2 \Phi_{\pm} + (\omega^2 - V_{\pm}(z)) \Phi_{\pm} = 0, \quad (3.37)$$

with $z'(r) = f(r)^{-1}$. The potentials $V_{\pm}(r)$ in (3.36) can only diverge at finite r if $H(r) = \vec{k}^2 r^2 - (n/2)r f'(r)$ goes to zero. Since $f'(r)$ is negative, this can only happen for negative \vec{k}^2 . So $V_{\pm}(r)$ is regular at finite r for $\vec{k}^2 \notin \mathbb{R}_-$. Also the UV asymptotics of the potentials follow (2.8) with $\nu^2 = (n-3)^2/4$ at finite momentum and $\nu^2 = (n+1)^2/4$ at $\vec{k} = 0$, which are both positive. We conclude that the variables Φ_{\pm} in (3.33) are associated with two-sided correlator $G_{12}^{\pm}(\omega, \vec{k})$ that obey the product formulae without zeroes, except potentially for negative \vec{k}^2 .

We would now want to relate the stress-tensor and current correlators to the master fields Green's functions $G^{\pm}(\omega, \vec{k})$. This relation depends on the dimensionality n , so we will now consider a fixed value of n . The case of $n = 2$ was treated in [3], where the sound channel correlators were found to be non-linearly related to G^{\pm} , as reviewed in appendix F. Here we will instead consider $n = 3$, for which the relation becomes linear. We argue in appendix F that this also holds for any $n \geq 4$.

The G^{\pm} correlators appear in the near-boundary expansion of the solutions to (3.37). The form of this expansion can be inferred from the behavior of $V_{\pm}(z)$ at $z \rightarrow 0$ ¹⁵

$$V_{\pm}(z) \underset{z \rightarrow 0}{\sim} \frac{(n-3)^2 - 1}{4z^2}, \quad (3.38)$$

$$\Phi_{+} = \frac{\vec{k}^2}{4nQ} \Phi_{-, \text{KI}} \quad , \quad \Phi_{-} = -\frac{\vec{k}^2}{(n+1)(M+\rho)} \Phi_{+, \text{KI}}.$$

¹⁵ V_{+} has a special behavior for $\vec{k} = 0$: $V_{+}(z) \sim n(n+2)/(4z^2)$. This case requires a special treatment, but can be computed by taking the limit of the finite \vec{k} result.

which implies

$$\underline{n \neq 3} : \Phi_{\pm}(z) = \Phi_{\pm}^{(0)} z^{\frac{4-n}{2}} (1 + \dots) + \Phi_{\pm}^{(1)} z^{\frac{n-2}{2}} (1 + \dots), \quad (3.39)$$

$$\underline{n = 3} : \Phi_{\pm}(z) = \Phi_{\pm}^{(0)} z^{\frac{1}{2}} \log z (1 + \dots) + \Phi_{\pm}^{(1)} z^{\frac{1}{2}} (1 + \dots). \quad (3.40)$$

where the dots refer to terms going to zero as $z \rightarrow 0$. For a solution of (3.37) with infalling boundary conditions at the horizon, we define the retarded correlator

$$G_R^{\pm}(\omega, k) = \frac{\Phi_{\pm}^{(1)}}{\Phi_{\pm}^{(0)}}, \quad (3.41)$$

and the two-sided correlator (see (2.3))

$$G_{12}^{\pm}(\omega, k) = \frac{\text{Im } G_R^{\pm}(\omega, k)}{\sinh(\beta\omega/2)}, \quad (3.42)$$

which obeys the product formula (2.4).

The stress tensor and current correlators that we are interested in, can them be related to the near-boundary expansion of the metric and gauge field in radial gauge ($n = 3$)

$$\delta g_{\mu\nu} = \frac{\ell^2}{r^2} \left(\delta g_{\mu\nu}^{(0)} + \delta g_{\mu\nu}^{(2)} r^2 + r^4 (\delta \pi_{\mu\nu} + \delta \psi_{\mu} \log r) \right), \quad (3.43)$$

$$\delta A_{\mu} = \delta A_{\mu}^{(0)} + r^2 (\delta \pi_{\mu} + \delta B_{\mu} \log r). \quad (3.44)$$

Up to contact terms, the retarded correlators are proportional to the ratio of the vev terms over the sources

$$\langle J_{\mu} J_{\nu} \rangle_R = C_J \frac{\delta \pi_{\mu}}{\delta A_{(0)}^{\nu}} + \text{contact terms}, \quad (3.45)$$

$$\langle T_{\mu\nu} T_{\alpha\beta} \rangle_R = C_T \frac{\delta \pi_{\mu\nu}}{\delta g_{(0)}^{\alpha\beta}} + \text{contact terms}, \quad (3.46)$$

$$\langle T_{\mu\nu} J_{\alpha} \rangle_R = C_{\text{mix}} \frac{\delta \pi_{\mu\nu}}{\delta A_{(0)}^{\alpha}} + \text{contact terms}, \quad (3.47)$$

for solutions of the Einstein-Maxwell equations with infalling boundary conditions at the horizon. C_J , C_T and C_{mix} are constants which only depend on the normalization of the bulk action. Since we are interested in the imaginary part of the retarded correlators, and because the contact terms are real, the latter will not be relevant to our discussion.

From the definitions (3.33), and using the near-boundary equations of motion¹⁶, the coefficients $\Phi_{\pm}^{(0)}$ and $\Phi_{\pm}^{(1)}$ can now be related to the metric and gauge field expansions (3.43)-(3.44) as

$$\Phi_{\pm}^{(0)} = -\frac{Q}{q} z_A + \frac{M \pm \rho(\vec{k})}{6Q} z_g, \quad (3.48)$$

¹⁶The latter imply in particular the Ward identities obeyed by the stress-tensor and current correlators (3.45)-(3.47). See [3] for more details of this calculation in the case $n = 2$.

$$\begin{aligned}\Phi_{\pm}^{(1)} = & -\frac{2Q}{q}\delta\pi_t + \frac{8(M \pm \rho(\vec{k}))}{Q\omega^2}\delta\pi_x^x + \frac{24(M \pm \rho(\vec{k}))}{\omega^2\vec{k}^2}\left(-\frac{Q}{q}z_A + \frac{M}{6Q}z_g\right) + \frac{M \pm \rho(\vec{k})}{12Q}z_g - \\ & -\frac{Q}{2}\delta g_t^{t(0)} + \left(\frac{4M(M \pm \rho(\vec{k}))}{Q\omega^2} + \frac{3Q}{4}\right)\left(\delta g_{y_1}^{y_1(0)} + \delta g_{y_2}^{y_2(0)}\right),\end{aligned}\quad (3.49)$$

where we defined the combinations of sources

$$z_A \equiv |\vec{k}|\left(|\vec{k}|\delta A_t^{(0)} + \omega\delta A_x^{(0)}\right), \quad (3.50)$$

$$z_g \equiv 2\vec{k}^2\delta g_t^{t(0)} - 4\omega|\vec{k}|\delta g_t^{x(0)} - 2\omega^2\delta g_x^{x(0)} + (\omega^2 - \vec{k}^2)\left(\delta g_{y_1}^{y_1(0)} + \delta g_{y_2}^{y_2(0)}\right). \quad (3.51)$$

The vev terms $\delta\pi_t$ and $\delta\pi_{xx}$ can then be expressed in terms of the G^{\pm} correlators by inverting the relations (3.41), which gives

$$\delta\pi_t = \frac{q}{4Q\rho(\vec{k})}\left[(M - \rho(\vec{k}))G_R^+\Phi_+^{(0)} - (M + \rho(\vec{k}))G_R^-\Phi_-^{(0)}\right] + \text{contact terms}, \quad (3.52)$$

$$\delta\pi_{xx} = \frac{\omega^2 Q}{16\rho(\vec{k})}\left[G_R^+\Phi_+^{(0)} - G_R^-\Phi_-^{(0)}\right] + \text{contact terms}. \quad (3.53)$$

Combined with the Ward identities, (3.52)-(3.53) finally makes it possible to express the retarded correlators (3.45)-(3.47) in terms of G_R^{\pm}

$$\langle J_a J_b \rangle_R = P_{ab}^{\parallel}(\omega, \vec{k})G_J(\omega, \vec{k}) + \text{contact terms}, \quad (3.54)$$

$$\langle T_{ab} T_{cd} \rangle_R = P_{ab}^{\parallel}(\omega, \vec{k})P_{cd}^{\parallel}(\omega, \vec{k})G_T(\omega, \vec{k}) + \text{contact terms}, \quad (3.55)$$

$$\langle T_{ab} T_{ii} \rangle_R = -\frac{1}{2}P_{ab}^{\parallel}(\omega, \vec{k})G_T(\omega, \vec{k}) + \text{contact terms}, \quad (3.56)$$

$$\langle (T_{y_1 y_1} + T_{y_2 y_2})T_{y_1 y_1} \rangle_R = \langle (T_{y_1 y_1} + T_{y_2 y_2})T_{y_2 y_2} \rangle_R = \frac{1}{2}G_T(\omega, \vec{k}) + \text{contact terms}, \quad (3.57)$$

$$\langle J_a T_{bc} \rangle_R = \frac{\omega^2 - \vec{k}^2}{2\vec{k}^2}\left(P_{ab}^{\parallel}(\omega, \vec{k})P_{tc}^{\parallel}(\omega, \vec{k}) + P_{ac}^{\parallel}(\omega, \vec{k})P_{tb}^{\parallel}(\omega, \vec{k})\right)G_{\text{mix}}(\omega, \vec{k}) + \text{contact terms}, \quad (3.58)$$

$$\langle J_a T_{ii} \rangle_R = -\frac{\omega^2 - \vec{k}^2}{2\vec{k}^2}P_{ta}^{\parallel}(\omega, \vec{k})G_{\text{mix}}(\omega, \vec{k}) + \text{contact terms}, \quad (3.59)$$

where a, b, c, d take values in (t, x) , whereas i, j take values in (y_1, y_2) (“ ii ” is not summed over). We introduced the longitudinal projector transverse to the 2-vector $k^a = (\omega, |\vec{k}|)$

$$P_{ab}^{\parallel}(\omega, \vec{k}) = \eta_{ab} + \frac{k_a k_b}{\omega^2 - \vec{k}^2}, \quad (3.60)$$

and defined the following combinations of master correlators

$$G_J(\omega, \vec{k}) \equiv C_J \frac{\omega^2 - \vec{k}^2}{4\rho(\vec{k})}\left[(M + \rho(\vec{k}))G_R^-(\omega, \vec{k}) - (M - \rho(\vec{k}))G_R^+(\omega, \vec{k})\right], \quad (3.61)$$

$$G_T(\omega, \vec{k}) \equiv C_T \frac{(\omega^2 - \vec{k}^2)^2}{48\rho(\vec{k})}\left[(M - \rho(\vec{k}))G_R^-(\omega, \vec{k}) - (M + \rho(\vec{k}))G_R^+(\omega, \vec{k})\right], \quad (3.62)$$

$$G_{\text{mix}}(\omega, \vec{k}) \equiv C_{\text{mix}} \frac{q\vec{k}^2(\omega^2 - \vec{k}^2)}{48\rho(\vec{k})} \left[G_R^+(\omega, \vec{k}) - G_R^-(\omega, \vec{k}) \right]. \quad (3.63)$$

Now taking the imaginary parts on both sides of equations (3.54)-(3.59) - and remembering that the contact terms are real - the sound channel two-sided correlators are found to be linearly related to the master correlators G_{12}^\pm . Since the latter obey the product formula, the stress tensor and current correlators can therefore also be written as a product over their poles. In particular, the G^- correlator has a diffusive pole $\omega_D(k) = -iD\vec{k}^2 + \mathcal{O}(\vec{k}^4)$, whereas G^+ features a sound pole $\omega_s(\vec{k}) = c_s|\vec{k}| - i\Gamma\vec{k}^2 + \mathcal{O}(\vec{k}^4)$ [29], as can be seen explicitly in the numerical results presented in appendix G. These results also indicate that the soft poles approach the IR poles in the near-extremal limit, as in (2.20). Following the discussion of section 2.3, in the near-extremal hydrodynamic regime we may therefore write the G^\pm correlators as

$$G_{12}^-(\omega, \vec{k}) = \frac{\gamma_-(\omega, \vec{k})\mathcal{G}_{12}^-(\omega, \vec{k})}{\omega^2 - \omega_D(\vec{k})^2}, \quad (3.64)$$

$$G_{12}^+(\omega, \vec{k}) = \frac{\gamma_+(\omega, \vec{k})\mathcal{G}_{12}^+(\omega, \vec{k})}{(\omega^2 - \omega_s(\vec{k})^2)(\omega^2 - \omega_s^*(\vec{k})^2)}, \quad (3.65)$$

with $\gamma_\pm(\omega, \vec{k})$ analytic in ω and free of zeroes (except potentially for $\vec{k}^2 < 0$), and $\mathcal{G}_{12}^\pm(\omega, \vec{k})$ the IR CFT₁ correlators (3.21), with conformal dimensions

$$\Delta_\pm(\vec{k}) = \frac{1}{2} \left(1 + \sqrt{5 + \frac{4\vec{k}^2 r_e^2}{n(n+1)}} \mp 4\sqrt{1 + \frac{4(n-1)\vec{k}^2 r_e^2}{n^2(n+1)}} \right). \quad (3.66)$$

Then, from (3.61)-(3.63) (and using (2.3)), the imaginary parts of the sound channel retarded correlators may themselves be written as product formulae

$$\text{Im}G_L(\omega, \vec{k}) = \frac{\gamma_L(\omega, \vec{k})\text{Im}\mathcal{G}_R^+(\omega, \vec{k})}{(\omega^2 - \omega_D(\vec{k})^2)(\omega^2 - \omega_s(\vec{k})^2)(\omega^2 - \omega_s^*(\vec{k})^2)}, \quad L \in \{T, J, \text{mix}\}, \quad (3.67)$$

with

$$\begin{aligned} \gamma_T(\omega, \vec{k}) \equiv & -C_T \frac{(\omega^2 - \vec{k}^2)^2}{48\rho(\vec{k})} \left((M + \rho(\vec{k}))\gamma_+(\omega, \vec{k})(\omega^2 - \omega_D(\vec{k})^2) - \right. \\ & \left. - (M - \rho(\vec{k})) \frac{\text{Im}\mathcal{G}_R^-(\omega, \vec{k})}{\text{Im}\mathcal{G}_R^+(\omega, \vec{k})} \gamma_-(\omega, \vec{k})(\omega^2 - \omega_s(\vec{k})^2)(\omega^2 - \omega_s^*(\vec{k})^2) \right), \end{aligned} \quad (3.68)$$

and similar expressions for γ_J and γ_{mix} . In particular, in the extremal hydrodynamic regime $T \ll |\omega|, |\vec{k}| \ll r_e^{-1}$, the IR correlators behave as $\text{Im}\mathcal{G}_R^\pm(\omega, \vec{k}) \sim \omega^{2\Delta_\pm(\vec{k})-1}$, from which we may infer the following properties:

- As expected [4], the leading order extremal hydrodynamic expressions

$$\text{Im}G_T \propto \frac{(\omega^2 - \vec{k}^2)^2}{|d(\omega, \vec{k})|^2} \omega^{2\Delta_+(\vec{k})-1} (\omega^2 + \mathcal{O}(r_e^4 \vec{k}^4)), \quad (3.69)$$

$$\text{Im}G_J, \text{Im}G_{\text{mix}} \propto \frac{(\omega^2 - \vec{k}^2)\vec{k}^2}{|d(\omega, \vec{k})|^2} \omega^{2\Delta_+(\vec{k})-1} (\omega^2 + \mathcal{O}(r_e^4 \vec{k}^4)) \quad (3.70)$$

$$d(\omega, \vec{k}) \equiv (\omega - \omega_D(\vec{k}))(\omega - \omega_s(\vec{k}))(\omega + \omega_s^*(\vec{k})),$$

agree with the extrapolation of leading order hydrodynamics to zero temperature [30], up to the modification of the low frequency power-law behavior from ω to $\omega^{2\Delta_+(\vec{k})-1}$;

- The contribution of the sound channel correlator G^+ always dominates over that of the diffusive channel correlator G^- for the stress-tensor and mixed correlators. For the current correlators, G^- only dominates for $r_e|\vec{k}| \ll r_e^2\omega^2$;
- For the energy-energy, density-density and energy-density spectral functions, the height of the sound peak is of order $\mathcal{O}((r_e|\vec{k}|)^{2\Delta_+(\vec{k})-3})$, whereas the diffusive peak is of order $\mathcal{O}((r_e|\vec{k}|)^{4\Delta_+(\vec{k})-2})$. This indicates that the diffusive peak is suppressed at low temperatures, as was observed in [28] for $n = 2$, and further provides the precise momentum scaling of this suppression in the extremal hydrodynamic regime. In particular, this scaling indicates that the diffusive peak tends to become more important as the momentum is increased, as was also observed in [28].

As a final remark, note that the ratio of the two IR correlators gives a power-law contribution $\omega^{2(\Delta_+(\vec{k})-\Delta_-(\vec{k}))}$ to the generalized susceptibility (3.68). The latter is an example of a non-analytic term in the extremal hydrodynamic expansion, which resums a series of logarithmic terms

$$(r_e\omega)^{2(\Delta_+(\vec{k})-\Delta_-(\vec{k}))} = (r_e\omega)^2 \left(1 + \frac{4(3n-4)}{3n^2(n+1)} (r_e\vec{k})^2 \log(r_e\omega) + \mathcal{O}(r_e^4 \vec{k}^4) \right). \quad (3.71)$$

3.3 Magnetized branes

For our last example, we consider a black brane background with $p = 3$, meaning that in the near-extremal regime the theory flows to a CFT_2 in the IR. A solution of this sort was found in [14], corresponding to a magnetized black brane at zero density. The action for the system is Einstein-Maxwell

$$S = \int dx^{d+1} \sqrt{-g} \left(R + \frac{d(d-1)}{\ell^2} - \ell^2 F_{MN} F^{MN} \right). \quad (3.72)$$

where the boundary dimension $d \geq 4$ is taken to be even, and ℓ is the AdS length. The field strength ansatz is of the form

$$F = B (dy_1 \wedge dy_2 + \cdots + dy_{d-3} \wedge dy_{d-2}). \quad (3.73)$$

with B the constant boundary magnetic field. An appropriate ansatz for the metric is then given by

$$ds^2 = e^{2A(r)} (-f(r)dt^2 + f(r)^{-1}dr^2 + h(r)dx^2 + dy_1^2 + \cdots + dy_{d-2}^2), \quad (3.74)$$

with r the radial coordinate, defined to be 0 at the AdS boundary, and x the direction of the magnetic field. The ansatz for the field strength (3.73) automatically solves the

Maxwell equations, whereas the Einstein equations may be written in terms of the ansatz fields (3.74) as

$$A''(r) - A'(r) \left(A'(r) + \frac{h'(r)}{2h(r)} \right) - \frac{f'(r)h'(r)}{2(d-1)f(r)h(r)} + \frac{2(B\ell)^2 e^{-2A(r)}}{(d-1)f(r)} = 0, \quad (3.75)$$

$$h''(r) + h'(r) \left((d-1)A'(r) + \frac{f'(r)}{f(r)} - \frac{h'(r)}{2h(r)} \right) - \frac{4(B\ell)^2 e^{-2A(r)} h(r)}{f(r)} = 0, \quad (3.76)$$

$$f(r)A'(r) \left(\frac{f'(r)}{f(r)} + \frac{h'(r)}{h(r)} + dA'(r) \right) + \frac{f'(r)h'(r)}{2(d-1)h(r)} - \frac{d e^{2A(r)}}{\ell^2} + \frac{d-2}{d-1} e^{-2A(r)} (B\ell)^2 = 0. \quad (3.77)$$

Equations (3.75)-(3.77) admit a BTZ $\times\mathbb{R}^{d-2}$ solution [14]

$$ds^2 = \left(\frac{\ell_3}{\rho} \right)^2 \left(-f_3(\rho) dt^2 + \frac{d\rho^2}{f_3(\rho)} + dx^2 \right) + \frac{B\ell^2}{\sqrt{d-1}} (dy_1^2 + \cdots + dy_{d-2}^2), \quad (3.78)$$

$$\rho = \frac{1}{\sqrt{d-1}} \frac{1}{B(r_0 - r)}, \quad (3.79)$$

where r_0 is an arbitrary integration constant, and the blackening function and AdS₃ length are given by

$$f_3(\rho) = 1 - \left(\frac{\rho}{\rho_h} \right)^2, \quad \ell_3 = \frac{\ell}{\sqrt{d-1}}, \quad (3.80)$$

with ρ_h the BTZ horizon radius.

The near-extremal magnetic brane solution [14] interpolates between the BTZ solution (3.78) near the horizon, and AdS_{d+1} in the UV. For the fields of the ansatz (3.74), this means that when the boundary is approached ($r \rightarrow 0$) the fields behave as

$$A(r) = -\log \left(\frac{r}{\ell} \right) + \mathcal{O}(r^4), \quad f(r) = 1 + \mathcal{O}(r^4), \quad h(r) = 1 + \mathcal{O}(r^4), \quad (3.81)$$

whereas near the horizon ($r \rightarrow r_H$) we have

$$A(r) = \frac{1}{2} \log \left(\frac{B\ell^2}{\sqrt{d-1}} \right) + \mathcal{O}(r_H - r), \quad (3.82)$$

$$f(r) = 4\pi T(r_H - r) + \sqrt{d-1} B(r_H - r)^2 + \mathcal{O}(r_H - r)^3, \quad (3.83)$$

$$h(r) = \frac{4\pi^2 T^2}{\sqrt{d-1} B} + 4\pi T(r_H - r) + \sqrt{d-1} B(r_H - r)^2 + \mathcal{O}(r_H - r)^3. \quad (3.84)$$

We now consider a probe neutral scalar field ϕ on the magnetic brane geometry, obeying the Klein-Gordon equation

$$\frac{1}{\sqrt{-g}} \partial_M (\sqrt{-g} g^{MN} \partial_N \phi) - m^2 \phi = 0. \quad (3.85)$$

The homogeneity of the background allows to expand ϕ in Fourier modes

$$\phi(r; x) = \int \frac{dk^d}{(2\pi)^d} e^{-i\omega t + ik_x x + ik_y y} \varphi_{\omega, k_x, k_y}(r), \quad (3.86)$$

where we took the momentum transverse to the magnetic field to lie in the $y \equiv y_1$ direction (without loss of generality). In Fourier space, (3.85) becomes

$$\begin{aligned} & e^{-(d-1)A(r)} h(r)^{-\frac{1}{2}} f(r) \partial_r \left(e^{(d-1)A(r)} h(r)^{\frac{1}{2}} f(r) \partial_r \varphi \right) + \\ & + \left(\omega^2 - \frac{f(r)}{h(r)} k_x^2 - f(r) k_y^2 - e^{2A(r)} f(r) m^2 \right) \varphi = 0, \end{aligned} \quad (3.87)$$

where the indices were suppressed on φ to avoid clutter. Introducing again the tortoise coordinates $dz/dr = 1/f(r)$, (3.87) may be put in Schrödinger form upon performing the field redefinition

$$\varphi(z) \rightarrow e^{-\frac{d-1}{2}A(z)} h(z)^{-\frac{1}{4}} \psi(z). \quad (3.88)$$

The field ψ obeys

$$\partial_z^2 \psi + (\omega^2 - V(z)) \psi = 0, \quad (3.89)$$

with the Schrödinger potential given by

$$\begin{aligned} V(z) = & f(z) \left(\frac{k_x^2}{h(z)} + k_y^2 + e^{2A(z)} m^2 \right) + \\ & + \frac{d-1}{2} A''(z) + \frac{d-1}{4} A'(z) \left((d-1) A'(z) + \frac{h'(z)}{h(z)} \right) - 3 \left(\frac{h'(z)}{4h(z)} \right)^2 + \frac{h''(z)}{4h(z)}. \end{aligned} \quad (3.90)$$

The potential (3.90) is regular everywhere and has UV asymptotics of the form (2.8) with $\nu^2 = (d-1)^2/4 \geq 0$, which ensures that the scalar two-sided correlator $G_{12}(\omega, k_x, k_y)$ associated with ϕ obeys the product formula without zeroes. The poles of the retarded correlator associated with ϕ can be computed from a numerical calculation, whose results are presented in appendix H. These results indicate that ϕ does not feature any gapless pole, and its soft poles approach the IR CFT₂ poles at low temperature. According to the discussion of section (2.3), the near-extremal limit of G_{12} may then be written as

$$G_{12}(\omega, k_x, k_y) = \gamma_e(\omega, k_x, k_y) \mathcal{G}_{12}^{k_y}(\omega, k_x), \quad (3.91)$$

with γ_e a function analytic in ω and free of zeroes, and $\mathcal{G}_{12}^{k_y}(\omega, k_x)$ the IR CFT₂^{k_y} correlator associated with ϕ . From the known expression for finite temperature CFT₂ two-point functions [12, 25], \mathcal{G}_{12} may be written in terms of the IR conformal dimension $\Delta(k_y)$ as

$$\mathcal{G}_{12}^{k_y}(\omega, k_x) = \frac{(2\pi T)^{2\Delta(k_y)-2}}{\pi \Gamma(\Delta(k_y) - 1)^2} \left| \Gamma \left(\frac{2\pi T \Delta(k_y) + i(\omega + k_x)}{4\pi T} \right) \right|^2 \left| \Gamma \left(\frac{2\pi T \Delta(k_y) + i(\omega - k_x)}{4\pi T} \right) \right|^2. \quad (3.92)$$

The dimension of the IR operator associated with ϕ can be read from the near-horizon limit of (3.87), which gives

$$\Delta(k_y) = 1 + \sqrt{1 + (m\ell_3)^2 + \frac{k_y^2}{\sqrt{d-1}B}}. \quad (3.93)$$

The extremal hydrodynamic product formula (2.19) is obtained from the zero-temperature limit of (3.92)

$$\text{Im}G_R(\omega, k_x, k_y) = \tilde{\gamma}_e(\omega, k_x, k_y)(r_e^2(\omega^2 - k_x^2))^{\Delta(k_y)-1}. \quad (3.94)$$

The zero-temperature effective susceptibility $\tilde{\gamma}_e$ is a function of $r_e^2(\omega^2 - k_x^2)$ and $r_e^2 k_y^2$, which is free of zeroes and analytic in its first argument.

4 An application to holographic neutrino transport

In this last section, the extremal hydrodynamic product formula (2.19) is applied to the setup considered in [7]. There, a toy model was introduced to investigate neutrino transport in holography, where the charged current spectral functions were computed from the Maxwell equations on the RN background, i.e. the problem considered in section 3.1. The numerical data for the spectral functions was then used to compute the neutrino and anti-neutrino opacities, κ and $\bar{\kappa}$. An interesting observation from this calculation was that the opacities at low temperatures were quite well approximated by substituting for the current correlators the leading order hydrodynamic expression [30], extrapolated to zero temperature.

As discussed in this work, the fact that the correlators can be approximated by a hydrodynamic expression is a direct consequence of the existence of a hydrodynamic-like gapless pole in the near-extremal regime (see appendix D), due to the product formula. In section 3.1, we further argued that the leading order extremal hydrodynamic product formula actually predicts expressions (3.19) and (3.24) which are slightly different from usual hydrodynamics. Specifically, the leading low-frequency behavior is changed from linear to $\omega^{2\Delta(k)-1}$, where $\Delta(k)$ is the momentum-dependent scaling dimension in the IR CFT₁. This specific power-law is the main signature on the spectral functions from the IR CFT, and from the branch-cut that arises in the zero-temperature limit. Here, we investigate how this improved description of the spectral functions affects the calculation of the neutrino opacities.

We first discuss how the change in the hydrodynamic expressions affects the approximation to the spectral functions themselves. This is presented in figure 2, which shows a comparison between, on the one hand, the relative difference of the exact (numerical) spectral functions with standard hydrodynamics (top), and with the extremal hydrodynamic expressions (3.19) and (3.24) (bottom), at $\mu/T \simeq 65$. As expected (see section 2.2), these plots indicate that the main effect of taking into account the IR dimension is to improve the description of the spectral functions at low frequency ω .

The better description of the correlators at low energies translates into a better approximation to the neutrino opacities, as illustrated in figures 3 and 4. The latter show a comparison of the exact holographic opacities with the hydrodynamic and extremal hydrodynamic approximations, as a function of neutrino energy E_ν and for two different values of the ratio of chemical potential to temperature¹⁷: $\mu_1/T \simeq 4.7$ and $\mu_2/T \simeq 65$. For most

¹⁷For $T = 10$ MeV, these values correspond to baryon number densities $n_{B,1} = 10^{-3}$ fm⁻³ and $n_{B,2} = 1$ fm⁻³, which covers the typical range expected in neutron stars [7].

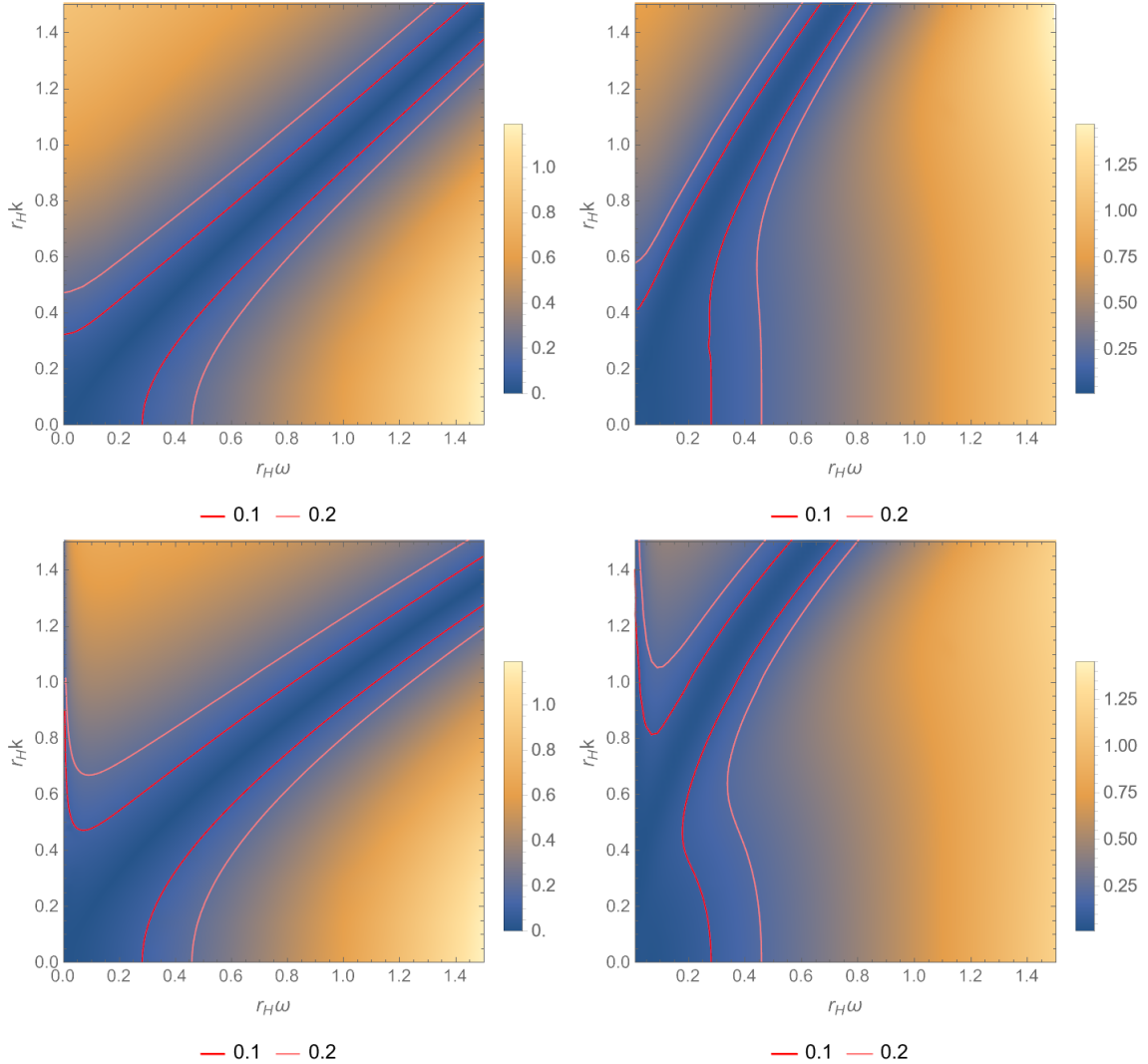


Figure 2: Relative difference of the numerically computed transverse (left) and longitudinal (right) spectral functions, with the leading order hydrodynamic (top) and extremal hydrodynamic (bottom) approximations. The relative differences are shown as a function of frequency ω and momentum $|\vec{k}|$, in units of the horizon radius r_H . The chemical potential to temperature ratio is $\mu/T \simeq 65$.

values of E_ν , the extremal and standard hydrodynamic approximations are observed to have similar accuracies, except near the dip in the neutrino opacity around $E_\nu \sim \mu_\nu$ (figure 3), where the extremal hydrodynamic approximation gives a significantly better description. This is consistent with expectations, since the integrand from which the neutrino opacity is computed (see [7]) is concentrated near $\omega = 0$ in this case. Note that this regime of neutrino energies is particularly important to describe well since it corresponds to the

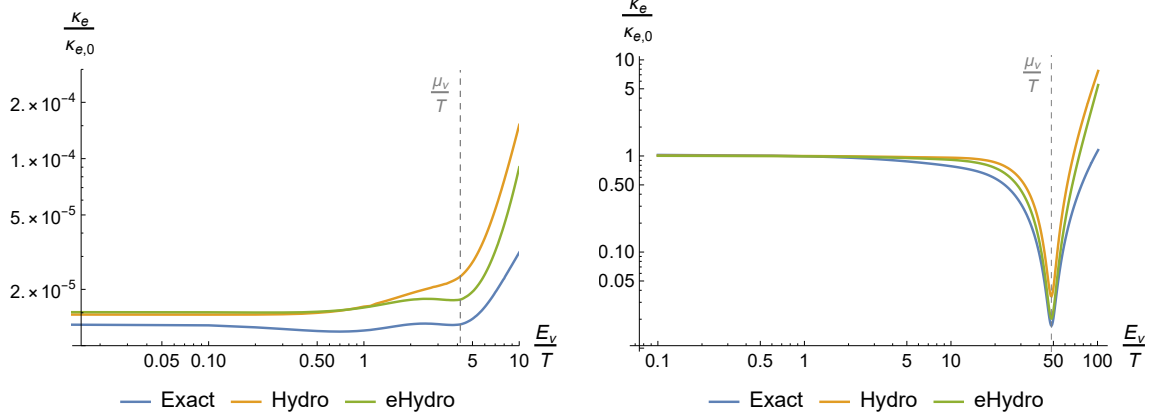


Figure 3: Neutrino opacity κ and its hydrodynamic approximations as a function of the neutrino energy E_ν , for $\mu/T \simeq 4.7$ (left) and $\mu/T \simeq 65$ (right). $\kappa_{e,0}$ is a normalization factor that was introduced in [7].

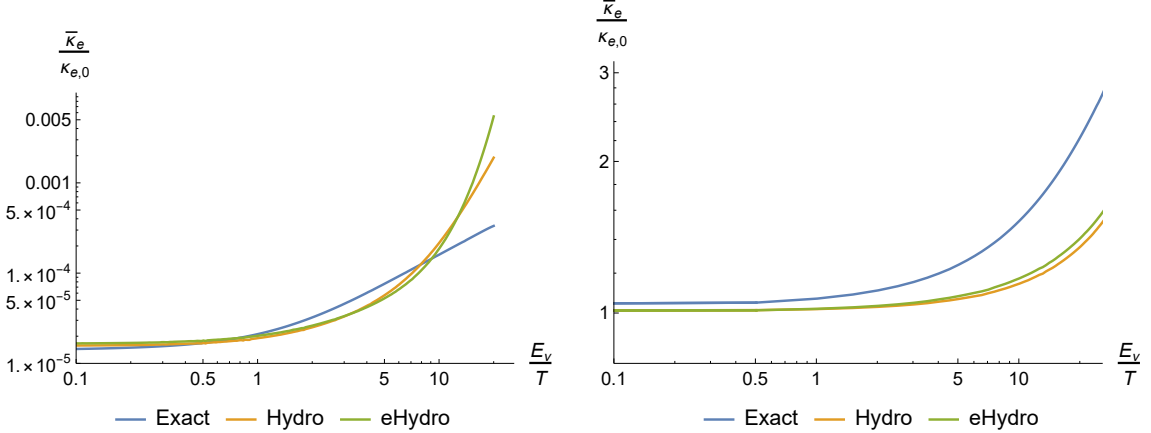


Figure 4: Same as figure 3 but for the anti-neutrino opacity $\bar{\kappa}$.

effective Fermi surface¹⁸, near which most neutrinos are emitted and absorbed.

5 Discussion

In this work, we used the holographic product formula introduced in [12] to get insight into the structure of holographic spectral functions in the near-extremal hydrodynamic regime, $\omega, k, T \ll \mu$. In the limit of vanishing temperature $T \ll \omega, k \ll \mu$, the formula provides an expression where both the low temperature gapless modes and the IR scaling behavior appear explicitly, moreover in a simple factorized form. As we showed in sections 3 and 4, the product formula applies in many holographic settings, where it allows to extend the near-extremal hydrodynamic approximation of correlators to the regime of low energies.

¹⁸See [7] for a discussion of the quasi-particle approximation considered for the description of neutrinos.

Several directions may be envisaged for future developments on this topic:

- Here we mostly focused on the pole structure, but also found in the various examples that the properties of the Schrödinger potential provide information on the zeroes of the spectral functions. It would be interesting to study further the relation between zeroes and singularities of the potential, especially since zeroes are typically much harder to compute than poles in holography;
- Another interesting point is related to the recent results of [31, 32] in four bulk dimensions, which showed that duality relations between different parity sectors of correlators translate into additional constraints on their structure. These may allow to write even more useful expressions in the near-extremal hydrodynamic regime of $(2+1)$ -dimensional holographic theories;
- In [12], the UV limit $\omega \gg T$ of the product formula was analyzed in relation with the OPE in the UV CFT. Here, we were rather interested in an IR regime of the correlators $\omega \ll \mu$, but also considered the limit $T \ll \omega \ll \mu$ to write the extremal hydrodynamic product formula. In this case, the corrections of order $\mathcal{O}(T/\omega)$ to the extremal result may still be controlled by an OPE, although rather associated with the IR CFT, which could be worth investigating;
- We focused on situations where the bulk fluctuation equations can be decoupled, especially since the IR correlator emerges simply in this case. Even when the equations cannot be decoupled, if the background geometry asymptotes to AdS_p near the horizon, then the low energy limit of correlators should still be controlled by the IR CFT. It would be nice to understand how this comes about in the more general coupled case, and generalize the near-extremal product formulae accordingly.

Finally, the main problem remains to understand what is the structure of the low energy effective field theory (EFT) that underlies the near-extremal spectral functions, which should combine both hydrodynamic-like features and the IR CFT. The formalism of [33–35] should a priori encompass this kind of theories, since it is well adapted to describe systems with hydrodynamic-like features [22]. This type of effective theories are also known to arise in holographic calculations [6, 36, 37], which however still remain to be extended to the relevant systems.

Acknowledgements

I would like to thank Andrew Gomes and Eren Firat for interesting discussions on the topic of this work. I am also grateful to Blaise Goutéraux and Jay Armas for useful comments on a draft. This project has received funding from the European Union’s Horizon 2024 research and innovation program under the Marie Skłodowska-Curie grant agreement No 101210184.

A IR limit of near-extremal correlators

In this appendix, we show how the near-extremal correlators computed from the Schrödinger equation

$$\psi''(z) + (\omega^2 - V(z))\psi(z) = 0, \quad (\text{A.1})$$

are related in the IR limit to correlators in the IR CFT_{p-1}. For general p , the IR limit is defined by

$$k_{p-1}^2 = -\omega^2 + \vec{k}_{p-2}^2 \rightarrow 0. \quad (\text{A.2})$$

Since the background is near-extremal, the temperature T is also much smaller than the scale μ , so the limit depends on the hierarchy between $|k_{p-1}|$ and T . We will consider the most general case where the two are of the same order¹⁹

$$k_{p-1}^2 \rightarrow \epsilon^2 k_{p-1}^2 \quad , \quad T \rightarrow \epsilon T \quad , \quad \epsilon \ll 1. \quad (\text{A.3})$$

Since the system becomes Lorentz invariant along the directions of the IR CFT at zero temperature, it is convenient to redefine the Schrödinger potential such that (A.1) takes the form

$$\psi''(z) + (\omega^2 - \vec{k}_{p-2}^2 - V(z))\psi(z) = 0. \quad (\text{A.4})$$

Now, the procedure to exhibit the relation with the IR correlator is based on the standard division of the bulk into inner and outer region [9, 10]:

- The inner region is where $z \gg 1$. Taking

$$z \equiv \epsilon^{-1}\zeta, \quad (\text{A.5})$$

with ϵ the same small parameter that appears in (A.3) and ζ of order 1, the near-extremal backgrounds of interest are such that the potential in (A.4) behaves as

$$V(z) \sim \epsilon^2 \zeta^{-2} V_p(\zeta T, \zeta^2 k_{p-1}^2, r_e^2 \vec{k}_{d-p+1}^2). \quad (\text{A.6})$$

The Schrödinger equation in the inner region then takes the form

$$\psi''(\zeta) - (k_{p-1}^2 + \zeta^{-2} V_p(\zeta))\psi(\zeta) = 0, \quad (\text{A.7})$$

which should be the equation of motion for a fluctuation in AdS_p-Schwarzschild. In particular, near the AdS_p boundary ($\zeta \rightarrow 0$), the dependence of V_p on the temperature and CFT momentum drops, so that (A.7) takes a homogeneous form

$$\psi''(\zeta) - \frac{\alpha(r_e^2 \vec{k}_{d-p+1}^2)}{\zeta^2} \psi(\zeta) = 0, \quad (\text{A.8})$$

which has two independent solutions

$$\psi_{\pm}(\zeta) = \zeta^{\frac{1}{2} \pm \nu(r_e^2 \vec{k}_{d-p+1}^2)} \quad , \quad \nu(r_e^2 \vec{k}_{d-p+1}^2) \equiv \frac{1}{2} \sqrt{1 + 4\alpha(r_e^2 \vec{k}_{d-p+1}^2)}. \quad (\text{A.9})$$

¹⁹Other cases can be obtained by taking appropriate limits of the result with $|k_{p-1}|$ and T of the same order.

By fixing the normalization of $\psi(z)$, we may therefore write the solution near the boundary of the inner region as

$$\psi(\zeta) = \zeta^{\frac{1}{2}-\nu}(1+\dots) + \mathcal{G}(\omega, \vec{k})\zeta^{\frac{1}{2}+\nu}(1+\dots), \quad (\text{A.10})$$

where the coefficient of the subleading term is the IR correlator by definition [9], and the dots go to zero as $\zeta \rightarrow 0$. Note that $\Delta_{\text{IR}} = 1/2 + \nu$ is (half) the scaling dimension of the IR correlator associated with ψ .

- The outer region is where $\zeta \ll 1$. In particular, it overlaps with the inner region near the boundary of the IR AdS_p , where the outer solution behaves as in (A.10). By linearity of (A.4), the full outer solution may then be written as [9]

$$\psi_{\text{out}}(z) = \eta_-(z) + \mathcal{G}(\omega, \vec{k})\eta_+(z). \quad (\text{A.11})$$

Near the UV boundary ($z \rightarrow 0$), $\eta_{\pm}(z)$ obeys an expansion controlled by (half) the dimension Δ_{UV} of the UV correlator associated with ψ , which takes the form

$$\eta_{\pm}(z) = a_{\pm}(\omega, \vec{k})z^{1-\Delta_{\text{UV}}}(1+\dots) + b_{\pm}(\omega, \vec{k})z^{\Delta_{\text{UV}}}(1+\dots), \quad (\text{A.12})$$

where the dots vanish at $z = 0$. The correlator associated with ψ may then be expressed as

$$G_{\psi}(\omega, \vec{k}) = \frac{b_-(\omega, \vec{k}) + b_+(\omega, \vec{k})\mathcal{G}(\omega, \vec{k})}{a_-(\omega, \vec{k}) + a_+(\omega, \vec{k})\mathcal{G}(\omega, \vec{k})}. \quad (\text{A.13})$$

Equation (2.16) in the main text is obtained from the expansion of the imaginary part²⁰ of (A.13) at small $r_e|\omega|$ and $r_e|\vec{k}|$, in the case where G is the retarded correlator (i.e. for ψ obeying infalling boundary conditions at the horizon).

B An example at next-to-leading order in the near-extremal hydrodynamic expansion

We discuss here how the correlator computed in [11] at next-to-leading order in the near-extremal hydrodynamic expansion fits with the product formula (2.14), and in particular with its extremal limit (2.19).

The correlator in question corresponds to the longitudinal retarded two-point function for a U(1) current in the neutral AdS_4 -black-brane state with metric²¹

$$\begin{aligned} ds^2 &= \frac{\ell^2}{r^2} \left(-f(r)dt^2 + f(r)^{-1}dr^2 + d\vec{x}^2 \right), \\ f(r) &= 1 - \frac{m^2 r^2}{2} - \left(1 - \frac{m^2 r_H^2}{2} \right) \frac{r^3}{r_H^3}, \end{aligned} \quad (\text{B.1})$$

²⁰Taking into account that η_{\pm} are real for real ω and \vec{k} .

²¹Note that this is the same problem as in section 3.1, only for a specific choice of the blackening function $f(r)$.

where ℓ is the AdS length, r_H the horizon radius and m the source for the two massless scalar fields that are also turned on in the background

$$\psi_i = mx^i, \quad i \in \{1, 2\}. \quad (\text{B.2})$$

In the regime

$$|\omega| \sim |\vec{k}^2|/m \sim T = \mathcal{O}(\epsilon)m, \quad \epsilon \ll 1, \quad (\text{B.3})$$

the result of [11] takes the form²²

$$G_{xx}^R(\omega, \vec{k}) = \frac{r_e^{-1}\omega^2 \left(1 - \frac{1}{3}\vec{k}^2\mathcal{G}\right) + \mathcal{O}(\epsilon^4)}{i\omega - \vec{k}^2 + \frac{1}{6}\vec{k}^2 \left(4\pi T + 2(\vec{k}^2 + i\omega)\mathcal{G} + 3\vec{k}^2 \log 3\right) + \mathcal{O}(\epsilon^3)}, \quad (\text{B.4})$$

$$\mathcal{G} \equiv \pi \cot\left(\frac{i\omega}{2T}\right) + \gamma + \psi\left(\frac{i\omega}{2\pi T}\right) - \log\left(\frac{9}{4\pi T}\right), \quad (\text{B.5})$$

with x the direction of the momentum \vec{k} , $r_e \sim m^{-1}$ the extremal horizon radius and bold fonts indicating quantities measured in units of r_e^{-1} , e.g. $\omega \equiv r_e\omega$. In (B.5), ψ is the digamma function and γ the Euler constant.

We are interested in the limit²³ $\omega/T \rightarrow \infty$, for which the product formula (2.14) simplifies according to (2.18), whereas (B.4)-(B.5) becomes (for ω off the negative imaginary axis)

$$G_{xx}^R(\omega, \vec{k}) = \frac{r_e^{-1}\omega^2 \left(1 - \frac{1}{3}\vec{k}^2\mathcal{G}_0\right) + \mathcal{O}(\epsilon^4)}{i\omega - \vec{k}^2 + \frac{1}{6}\vec{k}^2 \left(2(\vec{k}^2 + i\omega)\mathcal{G}_0 + 3\vec{k}^2 \log 3\right) + \mathcal{O}(\epsilon^3)}, \quad (\text{B.6})$$

$$\mathcal{G}_0 \equiv \gamma - i\frac{\pi}{2} + \log\left(\frac{2\omega}{9}\right). \quad (\text{B.7})$$

At this order equation (B.6) has two poles [11]

$$\omega_{\pm}(\vec{k}) = -i\vec{k}^2 + i\frac{2}{3}\vec{k}^4 \left(\log(2\vec{k}^2) + \gamma - \frac{5}{4}\log 3 \mp i\pi\right) + \mathcal{O}(\vec{k}^6). \quad (\text{B.8})$$

This result indicates that the leading order diffusive pole $\omega = -i\vec{k}^2$ splits into two at next-to-leading order.

The imaginary part of (B.6) can now be written in the form of the product formula (2.14)

$$\text{Im}G_{xx}^R(\omega, \vec{k}) = \frac{r_e^{-1}g(\omega, \vec{k})}{(\omega^2 - \omega_+(\vec{k})^2)(\omega^2 - \omega_-(\vec{k})^2)}, \quad (\text{B.9})$$

²²Note that we also need $i\omega/(2\pi T) \notin \mathbb{N}^*$ for \mathcal{G} in (B.5) to be finite. In other words, the expansion (B.4) breaks down when $i\omega/(2\pi T)$ is a positive integer.

²³Note that, in this case, the soft poles do not match the poles of the IR CFT correlator as in (2.20) [11]. There is therefore no simple expression of the form (2.23) for the correlator in the general near-extremal regime $|\omega| \sim |\vec{k}^2| \sim T \ll r_e^{-1}$. However, the extremal formula (2.19) still applies.

with the denominator given by

$$g(\omega, \vec{k}) = -\omega \left[\omega^2 + \vec{k}^4 - \frac{1}{3} \vec{k}^2 \left(2 \left(\omega^2 - \vec{k}^4 \right) \log \left(\frac{2\omega}{9} \right) + 8\vec{k}^4 \log \left(\frac{2\vec{k}^2}{9} \right) + 2\gamma\omega^2 + \vec{k}^4 (6\gamma + 3\log(3)) - 2\pi\vec{k}^2\omega \right) \right] + \mathcal{O}(\epsilon^5). \quad (\text{B.10})$$

Finally, to recover (2.19), we factor out the IR power-law in (B.10) as

$$g(\omega, \vec{k}) \equiv \omega^{2\Delta(\vec{k})-1} \gamma_e(\omega, \vec{k}), \quad (\text{B.11})$$

with the IR scaling dimension given in this case by [11]

$$\Delta(\vec{k}) = \frac{1}{2} + \frac{1}{2} \sqrt{1 + \frac{4}{3} \vec{k}^2}, \quad (\text{B.12})$$

and the generalized susceptibility γ_e identified as

$$\gamma_e(\omega, \vec{k}) = -(\omega^2 + \vec{k}^4) + \frac{1}{3} \vec{k}^2 \left(4\omega^2 \log(\omega) + 8\vec{k}^4 \log(\vec{k}^2) + 2\omega^2 \left(\gamma - \log\left(\frac{9}{2}\right) \right) + \vec{k}^4 (6\gamma - 9\log(3) + 6\log(2)) - 2\pi\vec{k}^2\omega \right) + \mathcal{O}(\epsilon^4). \quad (\text{B.13})$$

In particular, the $\vec{k}^6 \log \omega$ term from (B.10) is seen to have been absorbed into the IR power-law factor, such that at least at this order the extremal hydrodynamic expansion of γ_e remains valid in the limit of vanishing ω . It is plausible that the surviving $\omega^2 \vec{k}^2 \log(\omega)$ term could also be resummed into a power-law involving $\Delta(\vec{k})$, such as $\omega^{2\Delta(\vec{k})}$ or $\omega^{\Delta(\vec{k})+1}$.

Another special feature of (B.13) is the existence of a zero at $\omega = \vec{k}^2 = 0$. As mentioned in the main text, this zero has to be there to account for the fact that the two gapless poles (B.8) merge into a single diffusive pole at leading order in the hydrodynamic expansion. At leading order, the product formula (2.19) indeed predicts

$$\text{Im}G_{xx}^R(\omega, \vec{k}) = \frac{r_e^{-1} \omega^{2\Delta(\vec{k})-1} \gamma_e(0)}{\omega^2 + \vec{k}^4}, \quad (\text{B.14})$$

which can be checked to be implied from (B.9)-(B.13) at leading order, with $\gamma_e(0) = -1$.

C Correlators for different field variables in the probe longitudinal gauge sector

In this appendix, we demonstrate the relation (3.17) for the correlators Π^{\parallel} and G_{Ψ} , associated respectively to the longitudinal electric field E^{\parallel} and the alternative field variable

$$\Psi(r) = \frac{f(r) \partial_r E^{\parallel}}{r^{(d-3)/2} (\omega^2 - f(r) k^2)}. \quad (\text{C.1})$$

The correlators may be extracted from the near-boundary ($r \rightarrow 0$) expansion of the fields, which takes the form

$$E^{\parallel}(r) = E_{(0)} \left(1 - \frac{\omega^2 - \vec{k}^2}{2(d-4)} r^2 + \mathcal{O}(r^4) \right) + \\ + r^{d-2} \left(-a_d (\omega^2 - \vec{k}^2)^{\frac{d-2}{2}} E_{(0)} \log r + E_{(2)} (1 + \mathcal{O}(r^2)) \right), \quad (\text{C.2})$$

$$\Psi(r) = \frac{1}{4-d} E_{(0)} r^{\frac{5-d}{2}} (1 + \mathcal{O}(r^2)) + \\ + (d-2) r^{\frac{d-3}{2}} \left(-a_d E_{(0)} \log(r) (\omega^2 - \vec{k}^2)^{\frac{d-4}{2}} + \frac{E_{(2)}}{\omega^2 - \vec{k}^2} (1 + \mathcal{O}(r^2)) \right), \quad (\text{C.3})$$

with a_d a dimension-dependent number, which vanishes for odd d . Up to a normalization constant, the retarded polarization function is then defined as

$$\Pi_R^{\parallel} = \frac{E_{(2)}}{E_{(0)}}, \quad (\text{C.4})$$

for infalling boundary conditions at the horizon.

To identify the G_{Ψ} correlator, it is useful to introduce

$$\phi(r) = r^{\frac{d-1}{2}} \Psi(r), \quad (\text{C.5})$$

which behaves as an AdS scalar field near the boundary

$$\phi(r) = \phi_{(0)} r^{d-\Delta} (1 + \mathcal{O}(r^2)) + r^{\Delta} \left(\tilde{\phi}_{(0)} \log r + \phi_{(\Delta)} (1 + \mathcal{O}(r^2)) \right), \quad \Delta = d-2. \quad (\text{C.6})$$

For $d \geq 7$, the leading term $\phi_{(0)}$ is non-normalizable and should be identified as the source, so that G_{Ψ}^R is unambiguously identified as $G_{\Psi}^R = \phi_{(\Delta)} / \phi_{(0)}$. However, if $d \leq 6$, the dimension Δ is inferior to $(d+2)/2$, for which two possible quantizations are possible, depending on whether $\phi_{(0)}$ or $\phi_{(\Delta)}$ is treated as the source [38]. In this case, two zero-free product formulae may therefore be written: one for the two-sided correlator associated with $\phi_{(\Delta)} / \phi_{(0)}$, and the other for the inverse $\phi_{(0)} / \phi_{(\Delta)}$ [38]. However, it is not difficult to see that one of these formulae automatically implies the other.

So choosing, without loss of generality, G_{Ψ}^R as

$$G_{\Psi}^R = \frac{E_{(2)}}{(\omega^2 - \vec{k}^2) E_{(0)}} = \frac{\Pi_R^{\parallel}}{\omega^2 - \vec{k}^2}, \quad (\text{C.7})$$

again up to a normalization constant, implies that

$$G_{\Psi} \propto \frac{\Pi_{12}^{\parallel}}{\omega^2 - \vec{k}^2}, \quad (\text{C.8})$$

is free of zeroes.

D Poles of the probe current correlators

In this appendix, we present a numerical calculation of the low-lying (gapless and soft) poles of the RN probe current correlators discussed in section 3.1, in the near-extremal regime. We used for this the Mathematica package of [39]. The transverse and longitudinal sectors are discussed separately.

D.1 Transverse correlator

The transverse sector does not feature any gapless pole, and the soft poles are purely imaginary. The momentum dependence of the first few soft poles is shown in figure 5, for $d = 4$ and $r_e T = (50\pi)^{-1} \simeq 6.4 \times 10^{-3}$. This shows a very good agreement with the IR poles²⁴ (shown as the orange lines)

$$\omega_n^{IR}(\vec{k}) = -i2\pi T(\Delta(\vec{k}) + n), \quad \Delta(\vec{k}) = \frac{1}{2} + \frac{1}{2}\sqrt{1 + \frac{4}{d(d-1)}(r_e \vec{k})^2}, \quad (\text{D.1})$$

up to small corrections that can be checked to be of order $\mathcal{O}(r_e T)$.

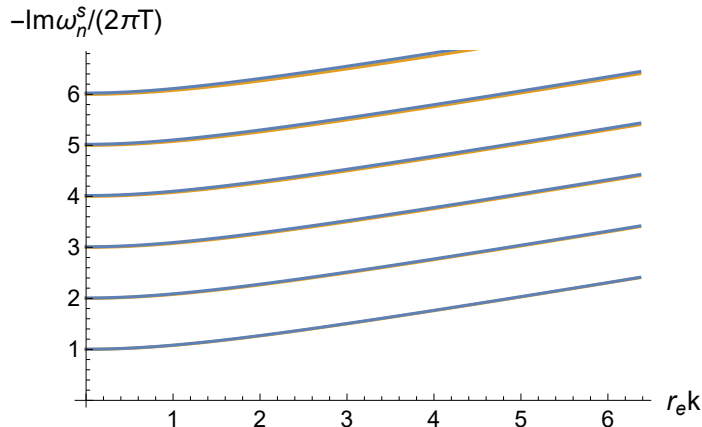


Figure 5: Imaginary part of the first soft poles of the transverse polarization function in units of $2\pi T$ and as a function of momentum $r_e |\vec{k}|$, for $d = 4$ and $r_e T = (50\pi)^{-1}$. The blue dots are the numerical results whereas the orange lines show the poles of the IR CFT₁ correlator (D.1).

D.2 Longitudinal correlator

We now present the numerical results for the poles of the longitudinal correlator, which are shown in figures 6 (imaginary part) and 7 (real part), still with $d = 4$ and $r_e T = (50\pi)^{-1}$. This sector contains both a diffusive pole $\omega_D(\vec{k}) = -iD\vec{k}^2 + \mathcal{O}(\vec{k}^4)$ and a sequence of soft poles, which interact non-trivially. The behavior as momentum increases is very similar to

²⁴The expression for the IR conformal dimension $\Delta(\vec{k})$ is obtained by substituting the RN blackening function (3.26) into (3.18).

[11], with the diffusive pole splitting into two poles with finite real parts before recombining on the imaginary axis several times as it collides with soft poles, before eventually remaining outside the imaginary axis, with a behavior of the form (B.8). Figure 6 indicates that the soft poles asymptote to the IR poles (D.1) (orange lines) at large momenta, but deviate significantly around the point where they cross the diffusive mode.

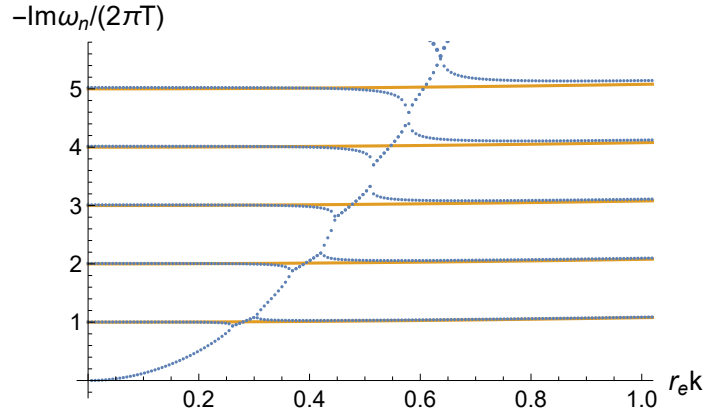


Figure 6: Imaginary part of the first low-lying poles of the longitudinal polarization function in units of $2\pi T$ and as a function of momentum $r_e |\vec{k}|$, for $d = 4$ and $r_e T = (50\pi)^{-1}$. The blue dots are the numerical results whereas the orange lines show the poles of the IR CFT₁ correlator (D.1).

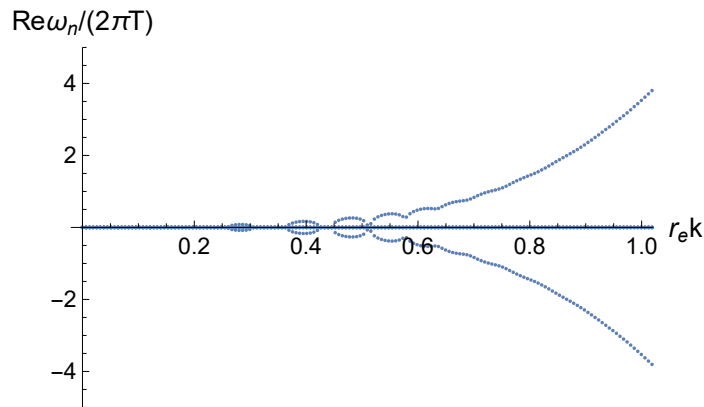


Figure 7: Real part of the poles shown in figure 6. For every momentum, at most two poles have finite real parts.

E Coefficients of the helicity-0 fluctuation equations

The coefficients appearing in (3.31)-(3.32) are given by

$$\zeta(r) \equiv r f'(r) - (n+1)(f(r) - 1), \quad (\text{E.1})$$

$$P_Z(r) \equiv -2\vec{k}^2 r^2 (rf'(r) + (n-2)f(r)) + nrf'(r) (rf'(r) - 5nf(r)) + 4n^2(n+1)f(r)(f(r) - 1), \quad (\text{E.2})$$

$$P_S(r) \equiv 4\vec{k}^2 r^2 \left(n(n-2)f(r) + \vec{k}^2 r^2 \right) - n^2 r f'(r) (rf'(r) - 2(2n+1)f(r)) - 4n^3(n+1)f(r)(f(r) - 1), \quad (\text{E.3})$$

$$V_S(r) = \frac{f(r)}{16r^2 H(r)^2} \left\{ 4\vec{k}^2 r^2 \left(4\vec{k}^4 r^4 + \right. \right. \\ + \vec{k}^2 r^2 (2(5n-4)rf'(r) + (8-7n(n+2))f(r) + 8n(n+1)) + \\ + n^2(19n-30)rf'(r)f(r) - n(n-4)r^2 f'(r)^2 - \\ - 8n^2(n+1)(2n-3)f(r)(f(r) - 1) \left. \right) + \\ + n^3 r f'(r) \left(((41n+26)f(r) - 8(n+1))rf'(r) - 10r^2 f'(r)^2 - \right. \\ - 16(n+1)(4n+1)f(r)(f(r) - 1) \left. \right) + \\ \left. + 32(n+1)^2 n^4 (f(r) - 1)^2 f(r) \right\}. \quad (\text{E.4})$$

F Stress-tensor correlators for other numbers of dimensions

In this appendix, we discuss the problem of section 3.2 for other numbers of dimensions, $n = 2$ and $n \geq 4$. We first review the case of $n = 2$, before considering $n \geq 4$.

F.1 $n = 2$

The helicity-0 correlators on the AdS₄-RN background were studied in [3]. As for $n = 3$, the system of fluctuation equations can be decoupled by considering the Kodama-Ishibashi (KI) master field Φ_{\pm} in (3.33). However, for $n = 2$, the relation between the near-boundary expansions of Φ_{\pm}

$$\Phi_{\pm}(r) = \Phi_{\pm}^{(0)}(1 + \mathcal{O}(r^2)) + \Phi_{\pm}^{(1)}r(1 + \mathcal{O}(r^2)), \quad (\text{F.1})$$

and the original metric and gauge field variables

$$\delta g^{\mu}_{\nu} = \delta g^{(0)\mu}_{\nu}(1 + \mathcal{O}(r^2)) + \delta \pi^{\mu}_{\nu} r^3(1 + \mathcal{O}(r^2)), \quad (\text{F.2})$$

$$\delta A_{\mu} = \delta A_{\mu}^{(0)}(1 + \mathcal{O}(r^2)) + \delta \pi_{\mu} r(1 + \mathcal{O}(r^2)), \quad (\text{F.3})$$

is such that the leading and subleading coefficients of Φ_{\pm} both contain a mixture of sources and vevs for the boundary operators. Explicitly [3]

$$\Phi_{\pm}^{(0)} = \frac{1}{\vec{k}^2} \left(-3r_H^2 \alpha_{\pm,0} \delta \pi_t^t - \vec{k}^2 \delta \pi_t + 4r_H^2 Q \alpha_{\pm,0}^2 \delta g^{(0)y}_y - \frac{1}{2} Q \vec{k}^2 \delta g^{(0)t}_t \right), \quad (\text{F.4})$$

$$\Phi_{\pm}^{(1)} = -\frac{4\alpha_{\pm}^0}{\vec{k}^4} \left(-3r_H^2 \alpha_{\pm,0} \delta \pi_t^t - \vec{k}^2 \delta \pi_t + 4r_H^2 Q \alpha_{\pm,0}^2 \delta g^{(0)y}_y - \frac{1}{2} Q \vec{k}^2 \delta g^{(0)t}_t \right) - \\ - \frac{1}{2} Q \alpha_{\pm}^0 \hat{z}_g - Q \hat{z}_a, \quad (\text{F.5})$$

where $\alpha_\pm^0 \equiv \alpha_\pm(r=0)$ (defined in (3.34)), and we defined

$$\hat{z}_a \equiv |\vec{k}|(|\vec{k}| \delta A_t^{(0)} + \omega \delta A_x^{(0)}) \quad (\text{F.6})$$

$$\hat{z}_g = \left[2\omega |\vec{k}| \delta g^{(0)x}_t + \omega^2 \delta g^{(0)x}_x - \vec{k}^2 \delta g^{(0)t}_t + (\vec{k}^2 - \omega^2) \delta g^{(0)y}_y \right]. \quad (\text{F.7})$$

Bold fonts indicate the quantities measured in units of the horizon radius r_H (e.g. $\omega \equiv r_H \omega$). Equations (F.4)-(F.5) imply that the helicity-0 correlators for $n=2$ cannot be linearly related to the the Kodama-Ishibashi correlators G^\pm .

As shown in [3], the stress-tensor and current correlators are instead linearly related to a different set of master variables, given by

$$\Psi_\pm \equiv \frac{4r_H^3 \alpha_\pm^0 Q}{\vec{k}^2} \Phi_\pm + f(r) r_H \partial_r \Phi_\pm. \quad (\text{F.8})$$

However, the Schrödinger potential associated with Ψ_\pm takes the form

$$V_\Psi^\pm(z) = V_\pm(z) - \frac{4Q\alpha_\pm^0}{\vec{k}^2} \frac{\gamma'_\pm(z)}{\gamma_\pm(z)} + \frac{\gamma''_\pm(z)}{2\gamma_\pm(z)} - \frac{(\gamma'_\pm)^2}{4\gamma_\pm^2}, \quad (\text{F.9})$$

with

$$\gamma_\pm(z) = \omega^2 - V_\pm(z) + \frac{16Q^2(\alpha_\pm^0)^2}{\vec{k}^4}. \quad (\text{F.10})$$

Since $V_\pm(z)$ is not always negative, the potential (F.9) will generically have singularities at finite z , implying that the correlators Π^\pm associated with Ψ_\pm may admit zeroes. Note that, from the definition (F.8), one can infer that the Π^\pm are related to the G^\pm as [3]

$$\Pi_R^\pm(\omega, \vec{k}) = r_H^{-1} \frac{a(\vec{k})^2 + \vec{k}^2 - \omega^2 + r_H a(\vec{k}) G_R^\pm(\omega, \vec{k})}{a(\vec{k}) + r_H G_R^\pm(\omega, \vec{k})}, \quad a(\vec{k}) \equiv \frac{4r_H^3 \alpha_\pm^0 Q}{\vec{k}^2}. \quad (\text{F.11})$$

F.2 $n \geq 4$

We now discuss the case where the number of boundary spatial dimensions is larger than 4. In this case, the near-boundary expansion of the KI fields takes the form

$$\Phi_\pm(r) = \Phi_\pm^{(0)} r^{1-\nu} (1 + \mathcal{O}(r^2)) + \Phi_\pm^{(1)} r^\nu (1 + \mathcal{O}(r^2)), \quad (\text{F.12})$$

with $\nu = (n-2)/2 \geq 1$. For the metric and gauge field we have

$$\delta g^\mu_\nu = \delta g^{(0)\mu}_\nu \left(1 + r^2 a_n(\omega, \vec{k}) + \mathcal{O}(r^4) \right) + r^{n+1} \left(b_n(\omega, \vec{k}) \delta g^{(0)\mu}_\nu \log r + \delta \pi^\mu_\nu (1 + \mathcal{O}(r^2)) \right), \quad (\text{F.13})$$

$$\delta A_\mu = \delta A_\mu^{(0)} \left(1 + c_n(\omega, \vec{k}) r^2 + \mathcal{O}(r^4) \right) + r^{n-1} \left(d_n(\omega, \vec{k}) \delta A_\mu^{(0)} \log r + \delta \pi_\mu (1 + \mathcal{O}(r^2)) \right), \quad (\text{F.14})$$

where b_n and d_n are 0 for even n . It can then be checked that $\Phi_\pm^{(0)}$ can be expressed in terms of the sources $\delta g^{(0)\mu}_\nu, \delta A_\mu^{(0)}$ only, without the vev's $\delta \pi^\mu_\nu, \delta \pi_\mu$. In this case, there are therefore linear relations between the stress-tensor and current correlators, and the KI correlators G^\pm .

G Poles of the stress-tensor correlators

We present in this appendix the results of a numerical calculation of the low-lying poles of the helicity-0 stress-tensor correlators analyzed in section 3.2, for $n = 3$ boundary spatial dimensions. The calculation was based on the Mathematica package of [39]. As discussed in section 3.2, the poles split into two families: the sound channel associated with the Φ^+ master variable, and the diffusive channel associated with Φ^- .

G.1 Diffusive channel

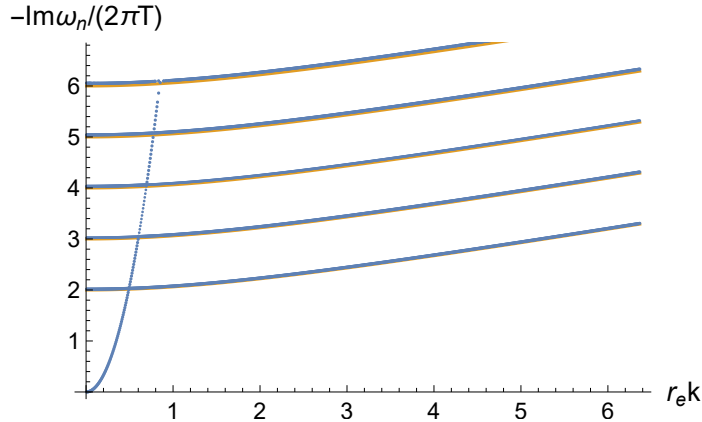


Figure 8: Imaginary part of the low-lying poles of the G^- retarded correlator, in units of $2\pi T$ and as a function of momentum $r_e |\vec{k}|$, for $n = 3$ and $r_e T = (50\pi)^{-1}$. The blue dots are the numerical results whereas the orange lines show the poles of the IR CFT₁ correlator (G.1).

Figure 8 shows the low-lying poles of the diffusive channel (which are purely imaginary), for $r_e T = (50\pi)^{-1} \simeq 6.4 \times 10^{-3}$. The behavior is identical to what was found in [6] for $n = 2$: there is a single gapless pole which is diffusive $\omega_D(\vec{k}) = -iD\vec{k}^2 + \mathcal{O}(\vec{k}^4)$, and, up to $\mathcal{O}(r_e T)$ corrections, the soft poles equal the IR poles (orange lines)

$$\omega_m^{\text{IR}}(\vec{k}) = -i2\pi T(\Delta_-(\vec{k}) + m), \quad (\text{G.1})$$

with the IR dimension given by (3.66).

G.2 Sound channel

The low-lying poles of the G^+ retarded correlator are shown in figures 9 (imaginary part) and 10 (real part), still for $n = 3$ and $r_e T = (50\pi)^{-1}$. Two sound poles $\omega_{s,\pm}(\vec{k}) = \pm c_s |\vec{k}| - i\Gamma \vec{k}^2 + \mathcal{O}(\vec{k}^4)$ are clearly identified, and the soft poles agree with the IR poles (orange lines in figure 9)

$$\omega_m^{\text{IR}}(\vec{k}) = -i2\pi T(\Delta_+(\vec{k}) + m), \quad (\text{G.2})$$

up to $\mathcal{O}(r_e T)$ corrections. Figure 10 also shows that the sound poles transition from hydrodynamic to relativistic behavior at large momentum, as has been observed previously for $n = 2$ [3].

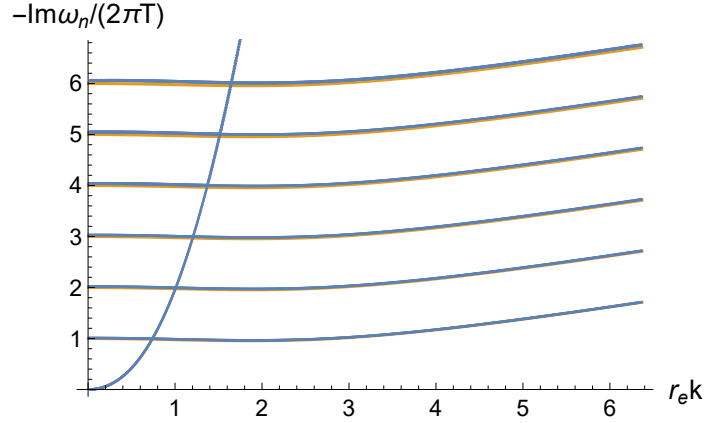


Figure 9: Imaginary part of the low-lying poles of the G^+ retarded correlator in units of $2\pi T$ and as a function of momentum $r_e|\vec{k}|$, for $n = 3$ and $r_e T = (50\pi)^{-1}$. The blue dots are the numerical results whereas the orange lines show the poles of the IR CFT₁ correlator (G.2).

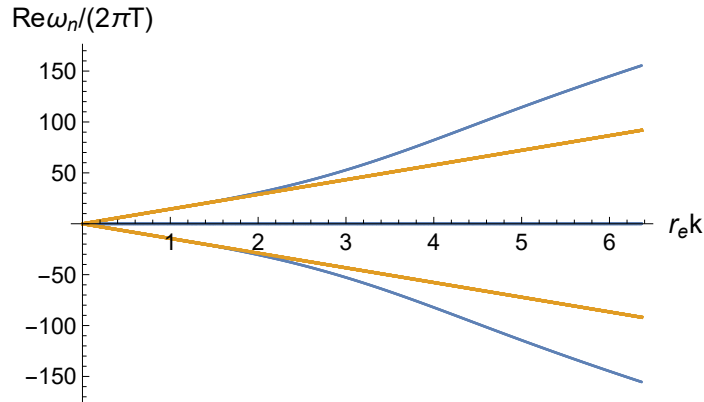


Figure 10: Real part of the poles shown in figure 9. Only the sound poles have finite real parts. The orange line shows the low momentum behavior $\omega_{s,\pm}^0(\vec{k}) = \pm c_s |\vec{k}| = \pm |\vec{k}|/\sqrt{n}$.

H Scalar poles of the magnetic black brane

We present in this appendix the results of a numerical calculation for the low-lying poles of the scalar correlator on the near-extremal magnetic black-brane background discussed in section 3.3. In this case the background itself is numerical, for which the package of [39] does not seem to handle higher working precision, which is necessary to compute more than the first two poles. Our calculation instead used a Mathematica script which is based on the same standard algorithm as [39], but allows to control the working precision throughout.

Figures 11, 12 and 13 present numerical results for the poles of a massless scalar at $r_e T \simeq 6.1 \times 10^{-3}$, with $r_e \sim B^{-1/2}$ the extremal horizon radius. Figure 11 shows the poles in the complex plane for a fixed value of the momentum $k_x = 2\pi T$ and $k_y^2 = \sqrt{d-1}B$,

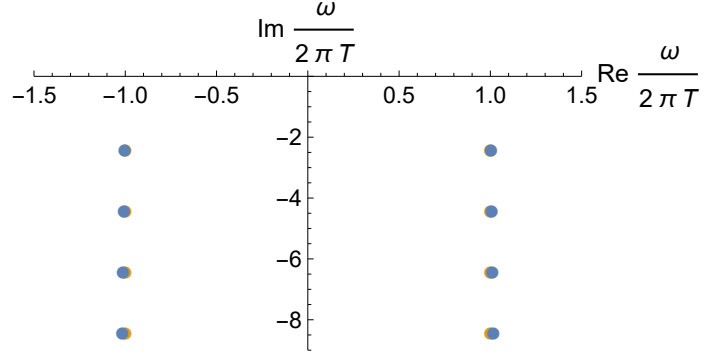


Figure 11: First four poles of the retarded correlator for a massless scalar on top of the near-extremal magnetic black-brane background, for $r_e T \simeq 6.1 \times 10^{-3}$, $k_x = 2\pi T$ and $k_y^2 = \sqrt{d-1}B$. The blue dots are the numerical results whereas the orange dots show the poles of the IR CFT₂ correlator (H.1).

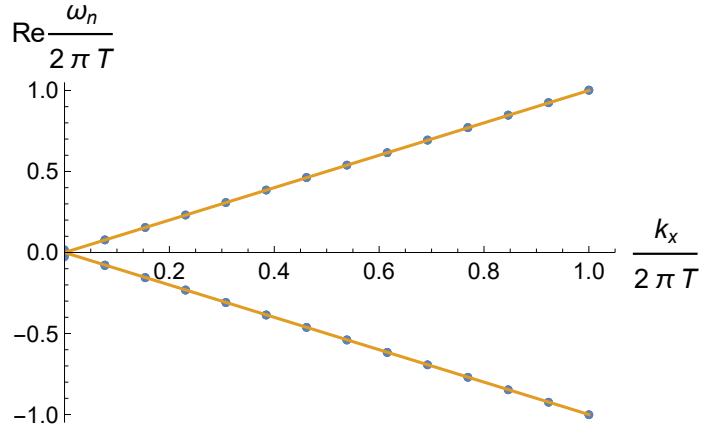


Figure 12: Evolution of the real part of the poles of figure 11 for $k_y = 0$ and k_x between 0 and $2\pi T$. The blue dots are the numerical results, which are compared to the poles of the IR CFT₂ correlator (H.1) (orange lines).

whereas the momentum dependence is displayed in figures 12 (k_x) and 13 (k_y). These results indicate that the low-temperature scalar poles approach the IR poles (shown in orange)

$$\omega_{n,\pm}^{\text{IR}}(k_x, k_y) = \pm k_x - i2\pi T(\Delta(k_y) + 2n), \quad (\text{H.1})$$

with $\Delta(k_y)$ given in (3.93).

References

[1] S. Bhattacharyya, V. E. Hubeny, S. Minwalla, and M. Rangamani, *Nonlinear Fluid Dynamics from Gravity*, *JHEP* **02** (2008) 045, [[arXiv:0712.2456](https://arxiv.org/abs/0712.2456)].

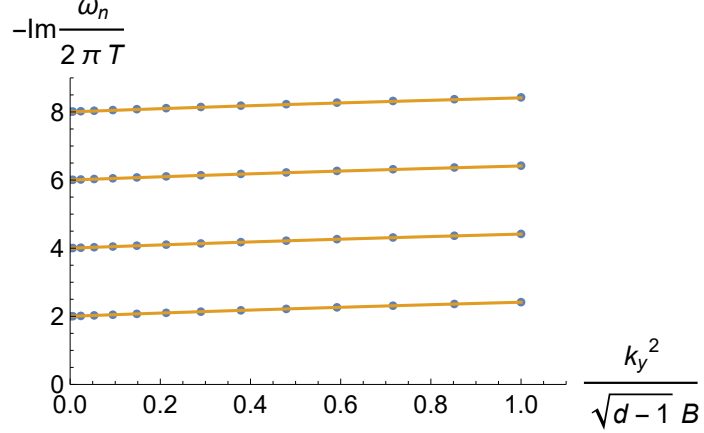


Figure 13: Evolution of the imaginary part of the poles of figure 11 for $k_x = 0$ and k_y between 0 and $\sqrt{d-1}B$. The blue dots are the numerical results, which are compared to the poles of the IR CFT₂ correlator (H.1) (orange lines).

- [2] M. Edalati, J. I. Jottar, and R. G. Leigh, *Shear Modes, Criticality and Extremal Black Holes*, *JHEP* **04** (2010) 075, [[arXiv:1001.0779](https://arxiv.org/abs/1001.0779)].
- [3] M. Edalati, J. I. Jottar, and R. G. Leigh, *Holography and the sound of criticality*, *JHEP* **10** (2010) 058, [[arXiv:1005.4075](https://arxiv.org/abs/1005.4075)].
- [4] U. Moitra, S. K. Sake, and S. P. Trivedi, *Near-Extremal Fluid Mechanics*, *JHEP* **02** (2021) 021, [[arXiv:2005.00016](https://arxiv.org/abs/2005.00016)].
- [5] R. A. Davison and A. Parnachev, *Hydrodynamics of cold holographic matter*, *JHEP* **06** (2013) 100, [[arXiv:1303.6334](https://arxiv.org/abs/1303.6334)].
- [6] R. A. Davison, B. Goutéraux, and E. Mefford, *Zero sound and higher-form symmetries in compressible holographic phases*, *JHEP* **12** (2023) 040, [[arXiv:2210.14802](https://arxiv.org/abs/2210.14802)].
- [7] M. Järvinen, E. Kiritsis, F. Nitti, and E. Préau, *Holographic neutrino transport in dense strongly-coupled matter*, *JHEP* **11** (2023) 139, [[arXiv:2306.00192](https://arxiv.org/abs/2306.00192)].
- [8] P. Arnaudo and B. Withers, *Exact low-temperature Green's functions in AdS/CFT: From the Heun equation to the confluent Heun equation*, *Phys. Rev. D* **111** (2025), no. 12 L121903, [[arXiv:2412.01923](https://arxiv.org/abs/2412.01923)].
- [9] T. Faulkner, H. Liu, J. McGreevy, and D. Vegh, *Emergent quantum criticality, Fermi surfaces, and AdS(2)*, *Phys. Rev. D* **83** (2011) 125002, [[arXiv:0907.2694](https://arxiv.org/abs/0907.2694)].
- [10] E. D'Hoker, P. Kraus, and A. Shah, *RG Flow of Magnetic Brane Correlators*, *JHEP* **04** (2011) 039, [[arXiv:1012.5072](https://arxiv.org/abs/1012.5072)].
- [11] B. Goutéraux, D. M. Ramirez, M. Sanchez-Garitaonandia, and C. Supiot, *Near-extremal holographic charge correlators*, [arXiv:2506.11974](https://arxiv.org/abs/2506.11974).
- [12] M. Dodelson, C. Iossa, R. Karlsson, and A. Zhiboedov, *A thermal product formula*, *JHEP* **01** (2024) 036, [[arXiv:2304.12339](https://arxiv.org/abs/2304.12339)].
- [13] J. Bhattacharya, N. Padhi, A. Sharma, and S. Singha, *Thermal Product Formula for Shear Modes*, [arXiv:2504.17781](https://arxiv.org/abs/2504.17781).

[14] E. D'Hoker and P. Kraus, *Magnetic Brane Solutions in AdS*, *JHEP* **10** (2009) 088, [[arXiv:0908.3875](https://arxiv.org/abs/0908.3875)].

[15] S. A. Hartnoll and S. P. Kumar, *AdS black holes and thermal Yang-Mills correlators*, *JHEP* **12** (2005) 036, [[hep-th/0508092](https://arxiv.org/abs/hep-th/0508092)].

[16] G. Festuccia and H. Liu, *Excursions beyond the horizon: Black hole singularities in Yang-Mills theories. I.*, *JHEP* **04** (2006) 044, [[hep-th/0506202](https://arxiv.org/abs/hep-th/0506202)].

[17] G. Festuccia, *Black hole singularities in the framework of gauge/string duality*, .

[18] D. Areán, I. Iatrakis, M. Järvinen, and E. Kiritsis, *The discontinuities of conformal transitions and mass spectra of V-QCD*, *JHEP* **11** (2013) 068, [[arXiv:1309.2286](https://arxiv.org/abs/1309.2286)].

[19] H. Kodama and A. Ishibashi, *Master equations for perturbations of generalized static black holes with charge in higher dimensions*, *Prog. Theor. Phys.* **111** (2004) 29–73, [[hep-th/0308128](https://arxiv.org/abs/hep-th/0308128)].

[20] Y. Bardoux, M. M. Caldarelli, and C. Charmousis, *Shaping black holes with free fields*, *JHEP* **05** (2012) 054, [[arXiv:1202.4458](https://arxiv.org/abs/1202.4458)].

[21] T. Andrade and B. Withers, *A simple holographic model of momentum relaxation*, *JHEP* **05** (2014) 101, [[arXiv:1311.5157](https://arxiv.org/abs/1311.5157)].

[22] M. Blake, H. Lee, and H. Liu, *A quantum hydrodynamical description for scrambling and many-body chaos*, *JHEP* **10** (2018) 127, [[arXiv:1801.00010](https://arxiv.org/abs/1801.00010)].

[23] M. Berkooz, A. Frishman, and A. Zait, *Degenerate Rotating Black Holes, Chiral CFTs and Fermi Surfaces I - Analytic Results for Quasinormal Modes*, *JHEP* **08** (2012) 109, [[arXiv:1206.3735](https://arxiv.org/abs/1206.3735)].

[24] H. F. Jia and M. Rangamani, *Holographic thermal correlators and quasinormal modes from semiclassical Virasoro blocks*, *JHEP* **12** (2024) 047, [[arXiv:2408.05208](https://arxiv.org/abs/2408.05208)].

[25] D. T. Son and A. O. Starinets, *Minkowski space correlators in AdS / CFT correspondence: Recipe and applications*, *JHEP* **09** (2002) 042, [[hep-th/0205051](https://arxiv.org/abs/hep-th/0205051)].

[26] P. Kovtun and A. Ritz, *Universal conductivity and central charges*, *Phys. Rev. D* **78** (2008) 066009, [[arXiv:0806.0110](https://arxiv.org/abs/0806.0110)].

[27] C. P. Herzog, P. Kovtun, S. Sachdev, and D. T. Son, *Quantum critical transport, duality, and M-theory*, *Phys. Rev. D* **75** (2007) 085020, [[hep-th/0701036](https://arxiv.org/abs/hep-th/0701036)].

[28] R. A. Davison and N. K. Kaplis, *Bosonic excitations of the AdS_4 Reissner-Nordstrom black hole*, *JHEP* **12** (2011) 037, [[arXiv:1111.0660](https://arxiv.org/abs/1111.0660)].

[29] D. Arean, R. A. Davison, B. Goutéraux, and K. Suzuki, *Hydrodynamic Diffusion and Its Breakdown near AdS_2 Quantum Critical Points*, *Phys. Rev. X* **11** (2021), no. 3 031024, [[arXiv:2011.12301](https://arxiv.org/abs/2011.12301)].

[30] P. Kovtun, *Lectures on hydrodynamic fluctuations in relativistic theories*, *J. Phys. A* **45** (2012) 473001, [[arXiv:1205.5040](https://arxiv.org/abs/1205.5040)].

[31] S. Grozdanov and M. Vrbica, *Duality and four-dimensional black holes: Gravitational waves, algebraically special solutions, pole skipping, and the spectral duality relation in holographic thermal CFTs*, *Phys. Rev. D* **112** (2025), no. 6 066019, [[arXiv:2505.14229](https://arxiv.org/abs/2505.14229)].

[32] S. Grozdanov and M. Vrbica, *Thermal field theory correlators in the large- N limit and the spectral duality relation*, [arXiv:2509.18074](https://arxiv.org/abs/2509.18074).

- [33] M. Crossley, P. Glorioso, and H. Liu, *Effective field theory of dissipative fluids*, JHEP **09** (2017) 095, [[arXiv:1511.03646](https://arxiv.org/abs/1511.03646)].
- [34] P. Glorioso, M. Crossley, and H. Liu, *Effective field theory of dissipative fluids (II): classical limit, dynamical KMS symmetry and entropy current*, JHEP **09** (2017) 096, [[arXiv:1701.07817](https://arxiv.org/abs/1701.07817)].
- [35] H. Liu and P. Glorioso, *Lectures on non-equilibrium effective field theories and fluctuating hydrodynamics*, PoS TASI2017 (2018) 008, [[arXiv:1805.09331](https://arxiv.org/abs/1805.09331)].
- [36] D. Nickel and D. T. Son, *Deconstructing holographic liquids*, New J. Phys. **13** (2011) 075010, [[arXiv:1009.3094](https://arxiv.org/abs/1009.3094)].
- [37] P. Glorioso, M. Crossley, and H. Liu, *A prescription for holographic Schwinger-Keldysh contour in non-equilibrium systems*, [arXiv:1812.08785](https://arxiv.org/abs/1812.08785).
- [38] I. R. Klebanov and E. Witten, *AdS / CFT correspondence and symmetry breaking*, Nucl. Phys. B **556** (1999) 89–114, [[hep-th/9905104](https://arxiv.org/abs/hep-th/9905104)].
- [39] A. Jansen, *Overdamped modes in Schwarzschild-de Sitter and a Mathematica package for the numerical computation of quasinormal modes*, Eur. Phys. J. Plus **132** (2017), no. 12 546, [[arXiv:1709.09178](https://arxiv.org/abs/1709.09178)].